Impact of Accelerated Stress Conditions on the Durability of Gas Diffusion Layers in Polymer Electrolyte Membrane Fuel Cells

A Major Qualifying Project Report
Submitted to the faculty of
WORCESTER POLYTECHNIC INSTITUTE
In partial fulfillment of the requirements for the
Degree of Bachelor of Science

Submitted to:
Stephen Kmiotek

By:
Samuel Bergström
Brent Young

April 27th, 2016

Co-Advised by:
François Lapicque (ENSIC)
Mariem Belhadj (ENSIC)

Abstract

This project, performed in conjunction with École Nationale Supérieure des Industries Chimiques (ENSIC) and Laboratoire Réactions et Génie des Procédés (LRGP) at the University of Lorraine in Nancy, France, focused on determining the causes of gas diffusion layer (GDL) degradation in proton exchange membrane (PEM) fuel cells and the effect of degradation of overall fuel cell performance. Our research determined that the main cause of GDL degradation is the presence of high potential across the fuel cell. GDL degradation was found to adversely affect fuel cell performance due to reduced effectiveness of water removal which leads to increased mass transport losses.

Acknowledgements

Table of Contents

Table of Figures

Introduction

As the attention paid to the environmental impacts of burning fossil fuels grows, an increased emphasis is being placed on the development of alternate forms of energy production. Fuel cells are a popular, and potentially viable, alternative to the combustion engine. Fuel cells are electrochemical devices with the ability to produce electricity by means of oxidation and reduction reactions. Fuel cell technology, by itself, cannot replace fossil fuels. Though the only product of fuel cell operation is water, a steady supply of fuel, generally in the form of hydrogen, is needed to produce electricity. As of now, the majority of hydrogen fuel is derived from hydrocarbons. In time, sufficient technology may develop to allow for alternative sources of hydrogen fuel. The potential advantage that fuel cells have over combustion engines is that their efficiency is not constrained by Carnot's Theorem. This translates to a greater energy output per unit of fuel and thus less consumption of hydrocarbons.

The main challenge facing fuel cell technology is cost. This issue is two-fold, with high initial production costs as well as a relative lack of durability which reduces the life of a cell. Great improvements have been made in fuel cell design to minimize the amount of high-cost materials required which have drastically reduced the cost of construction, though fuel cells still remain relatively expensive to produce. The issue of durability, on the other hand, still plagues fuel cells and is the center of the majority of the research performed on fuel cell technology.

This Major Qualifying Project (MQP) report is focused on performing multiple degradation test variations to analyze and determine the causes of fuel cell degradation and its effect on overall fuel cell performance. Two in situ experiments, cycling and carbon corrosion, and two ex situ

experiments, electrochemical degradation and immersion, were performed and the cells and/or membranes subsequently characterized. The characterization tests performed included chronopotentiometry (CP), electrochemical impedance spectroscopy (EIS), cyclic voltammetry (CV), and linear sweep voltammetry (LSV). Chronoamperometry (CA) was also performed, though during conditioning of a membrane.

This paper opens with an in-depth background on current fuel cell technology and the testing techniques employed in our experiments. Equipment and procedures are described in the following section. Finally, our findings and analyze the experimental results are presented. Supporting documents and complete data can be found in the appendices.

Background

Fuel cells are electrochemical power sources that generate electrical energy through the consumption of a fuel. Unlike heat engines, fuel cells rely on catalytic and porosity properties to generate an electric current from the combination of the fuel and an oxidizer. Fuel cells have the potential to operate at a higher efficiency than current heat engines while producing no greenhouse gas emissions, provided that the hydrogen supply is properly sourced. However, current fuel cell technology faces several hurdles before becoming a viable power source. Fuel cells are still expensive to manufacture and rapid degradation severely limits consistent efficiency and overall cell life. Scientists are currently working to resolve these issues.

Fuel Cell Basics

A fuel cell requires a steady supply of fuel to operate. The most common fuel used by the different types of fuel cells is hydrogen gas. The fuel gas is fed into the cell at the anode, coming in contact

with the catalyst layer. The platinum catalyst weakens the bonds of the fuel gas particles, causing protons to form. When this occurs, electrons are released in an excited state. The protons pass through the membrane while the electrons travel through the circuit connecting the anode to the cathode of the fuel cell. The movement of electrons through the circuit creates the desired current. The electrons and protons arriving at the cathode are joined by oxygen molecules, generally introduced through a flow of air at the cathode side of the cell. At the cathode, another catalyst layer causes the electrons and hydrogen ions to react with the oxygen molecules to form water. This reaction completes the circuit, resulting in the only products of the fuel cell being water heat. The overall reaction of the fuel cell is depicted as:

$$2H_2 + O_2 \rightarrow 2H_2O + \text{Heat}$$
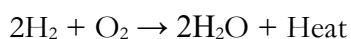
The reactions that fuel cells rely on to produce electricity proceed at a relatively slow rate, so fuel cells operate at higher temperatures and/or in the presence of a catalyst. Higher operating temperatures serve to provide the system with the energy required to more quickly overcome the activation energy necessary for a reaction to proceed. Catalysts lower the activation energy of the reaction, making it proceed at an increased rate and in a more energy efficient manner. When an otherwise stable molecule comes in contact with an active catalyst site, the bonding forces of the catalyst weaken the internal bonds of the molecule, making it more susceptible to reaction. The catalyst layer on the anode side of the cell serve to weaken the bond of fuel gas molecules, encouraging them to separate into two protons and an electron. The hydrogen protons proceed through the membrane while the electron transits through an external circuit, thus creating a current. The main part of the reaction in the cell, the "combustion" of fuel gas, takes place at the catalyst layer on the cathode side where the protons from the anode are oxidized. Upon moving through the membrane, protons encounter oxygen molecules with weakened bonds caused by the presence of platinum as well as the electrons that passed through the external circuit. These circumstances

facilitate the oxidization of the protons. For most types of fuel cells, the process is considered reverse electrolysis - water is formed from hydrogen and oxygen with an electric current produced in the process (Larminie and Dicks 2003).

The electrons produced at the anode produce a current along the external circuit that transports the electrons from the anode to the cathode. When no electrical work is being performed by the cell, the current is zero. At this state, referred to as an open circuit, the maximum achievable voltage potential, or open circuit voltage (OCV), is achieved. In an ideal system, OCV would be 1.23 V for a single fuel cell. However, due to ohmic resistances, mass transport limitations, and electrode capacitance the OCV of a cell is generally a few hundred mV lower than this. For commercial applications, multiple fuel cells must be combined in series to provide the necessary aggregate voltage.

History of Fuel Cells

The basic concept of fuel cell technology was first demonstrated in 1839 by William Robert Grove. This rudimentary fuel cell was comprised of two platinum electrodes, immersed in a dilute acid electrolyte solution, connected by an electric circuit. A power source was used to perform water hydrolysis which produced hydrogen and oxygen. An ammeter was then introduced into the system in place of the power source and small electric current was detected as a result of reverse electrolysis forming water from oxygen and hydrogen.

After Grove's discovery, a heated debate arose within the scientific community about how a current was created in a gas battery. While Grove and many others argued that electricity in the cell was created from a chemical reaction, a number of other scientists instead favored the theory that it was the physical contact of materials that facilitated the current. In truth, both theories were partially correct since electric current is created when chemical reactions take place at the contact points

between reactants, the electrolyte, and catalyst. In 1893, physical chemist Friedrich Wilhelm Ostwald furthered the field of fuel cell research by experimentally determining the functions of fuel cell components (Smithsonian Institution n.d.).

From 1880 to 1965, steady advances were made in fuel cell membrane technology. Solid electrolyte membranes were developed in place of liquid electrolyte solutions. Despite these improvements, high costs and low yields prevented fuel cells from becoming viable alternatives to hydroelectric power and traditional heat engines in any market. Then, in 1958 Francis Thomas Bacon demonstrated an operational fuel cell that employed an alkali electrolyte rather than a traditional acid electrolyte. Though still expensive to manufacture, the cell solved many reliability issues and was licensed by Pratt & Whitney to be used on the Apollo spacecraft (Smithsonian Institution n.d.).

PEM Fuel Cell History

In the early 1960s, Thomas Grubb and Leonard Niedrach developed PEM technology at General Electric in conjunction with the U.S. Navy Bureau of Ships and the U.S. Army Signal Corps. Despite being compact, portable, and able to operate at lower temperatures, the large amount of platinum catalyst required made PEM fuel cells expensive to produce. NASA employed PEM fuel cells on Gemini space missions. These cells were plagued with technical difficulties and NASA eventually transitioned to alkali fuel cells for subsequent space flights. In the 1970s, PEM water electrolysis technology developed by GE was adopted by the navies of the United States and Great Britain for their submarine fleets (Smithsonian Institution n.d.).

Types of Fuel Cells

There are currently six main recognized types of fuel cells in existence. Different fuel cell technologies have been created in response to different needs within the energy industry and each

have specialized mechanisms and functionalities. These fuel cells and their respective characteristics are shown in Table 1 and discussed in greater detail below.

Fuel Cell Type	Mobile Ion	Operating Temperature	Applications
Alkaline (AFC)	OH^-	50-200°C	Used in space vehicles
Proton exchange membrane (PEMFC)	H^+	30-100°C	Vehicles/mobile applications; lower power CHP systems
Direct methanol (DMFC)	H^+	20-90°C	Portable electronic systems of low power/long running times
Phosphoric acid (PAFC)	H^+	~220°C	High power CHP systems
Molten carbonate (MCFC)	CO_3^{2-}	~650°C	Medium- to large-scale CHP systems
Solid oxide (SOFC)	O^{2-}	500-1000°C	All CHP system sizes

Table 1: Fuel Cell Type Characteristics (Larminie and Dicks 2003)

Alkaline Fuel Cells (AFCs): This fuel cell type uses an electrolyte of potassium hydroxide (KOH) at varying concentrations dependent on the operating temperature, which ranges from 50-200°C (Larminie and Dicks 2003). The KOH electrolyte is contained in a matrix, generally made of asbestos. AFCs can use various electrocatalysts such as nickel, silver, metal oxides, and noble metals. AFCs will not perform properly in the presence of carbon dioxide (CO_2) at the anode or cathode. Use of AFCs has mostly been relegated to space flight since its commercialization in the 1960s (Barbir 2013).

Polymer Electrolyte Membrane/Proton Exchange Membrane Fuel Cells (PEMFCs):

PEMFCs use a conductive polymer membrane and a supported platinum catalyst on both the anode and cathode side of the cell. Currently, the loading concentration of platinum is approximately 0.3

mg/cm^2 (Barbir 2013). Current PEMFC research is focused on developing the technology for automotive applications to compete with current EVs on the market as well as the ability to function as small-scale backup electric generators (Barbir 2013).

Direct Methanol Fuel Cells (DMFCs): These fuel cells operate in much the same way as PEMFCs with the distinction being the type of fuel used. As the name suggests, DMFCs use methanol in the place of hydrogen which is used by most other types of fuel cells. Because of this, DMFCs produce carbon dioxide as a byproduct of electrical production. This type of cell produces very low power, but has the advantage of not requiring the formation of hydrogen as a prerequisite to operation. DMFC technology is being developed for applications requiring slow, steady electrical production (Larminie and Dicks 2003).

Phosphoric Acid Fuel Cells (PAFCs): PAFCs use an electrolyte of concentrated phosphoric acid retained in a SiC matrix. An electrocatalyst of platinum is present at both the anode and cathode (Barbir 2013). These fuel cells operate at a temperature range of 150°C and 220°C and have been commercialized as stationary electricity generators chiefly by United Technologies Research Center, however the company's fuel cell operations have subsequently been purchased by Doosan Fuel Cell.

Molten Carbonate Fuel Cells (MCFCs): MCFCs utilize an electrolyte comprised of a mixture of alkali carbonates retained in a ceramic matrix of $LiAlO_2$. At optimal high operating temperatures, the electrolyte forms a highly conductive molten salt with ionic conduction sustained with carbonate ions. With such high operating temperatures, a catalyst is generally not needed in these fuel cells. MCFCs are currently in the research and development phase with potential for stationary power generation (Barbir 2013).

Solid Oxide Fuel Cells (SOFCs): SOFCs use solid, nonporous metal oxide as an electrolyte. Operating at temperatures up to 1,000°C, ionic conduction by oxygen ions takes place. This type of

fuel cell is in the research and development phase with potential applications in both stationary

power generation and portable primary or auxiliary power in automobiles (Barbir 2013).
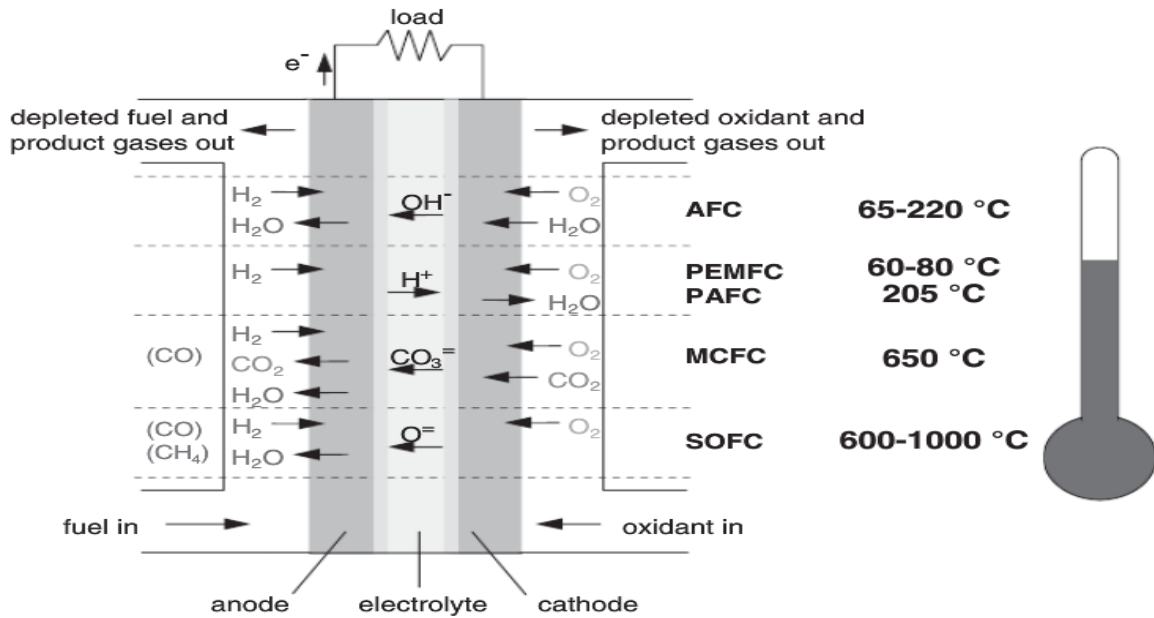
Figure 1: Internal Reactions of Fuel Cell Types (Barbir 2013)

Proton Exchange Membrane Fuel Cell Principles

PEMFCs are comprised of a two major parts: the membrane electrode assembly (MEA) and two

bipolar plates. In this section, we will discuss the properties and functions of all PEMFC

components and the theories and principles that govern their design.
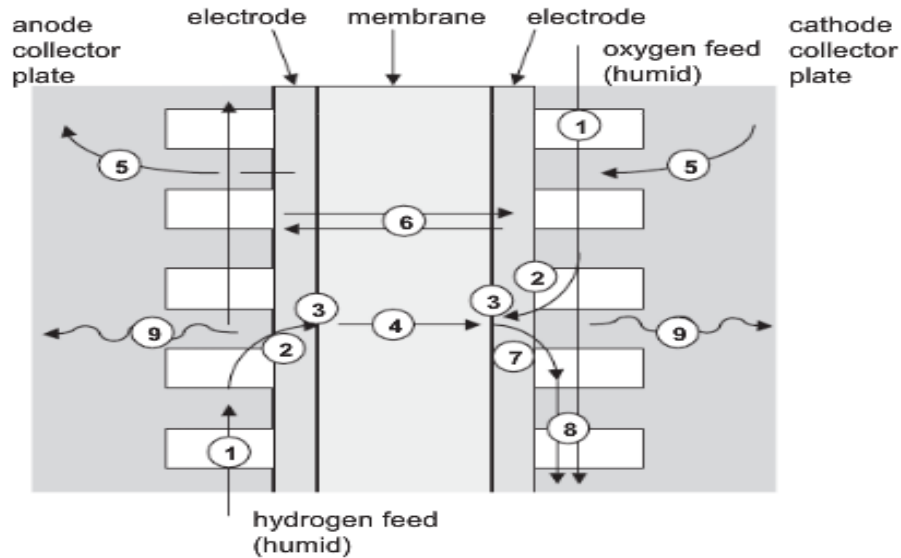
Figure 2: Depiction of fuel cell components and internal process (Barbir 2013)

Membrane Electrode Assembly (MEA)

The MEA is the main part of the PEM fuel cell and is comprised of a proton conductive membrane sandwiched between two electrodes. Each electrode consists of a catalyst layer. The MEA facilitates the transport of hydrogen and oxygen from the bulk gas flow to the interface between the electrodes and membrane where the reduction and oxidation reactions occur.

Polymer Electrolyte Membrane (PEM)

The polymer electrolyte membrane, also known as the proton exchange membrane, is the identifying characteristic of PEM fuel cells. The membrane separates the oxidation and reduction reactions at the cathode and anode, respectively. The ideal membrane is impermeable to electrons and diatomic hydrogen molecules, yet porous to water and protons (lone hydrogen nuclei). Nafion®, made by DuPont, is the most commonly used PEM and is composed of a perfluorosulfonic acid (PFSA) polymer. PFSA polymers are made from a polytetrafluoroethylene (PTFE, or Teflon) polymer main chain with side chains ending in sulfonic acid groups. These side chains are acidic ionomers which

13

terminate with easily dissociating SO_3H groups (becoming SO_3^- and H^+). Other structural variations (different polymer backbones) are used and developed, however the PSFA model is the most widely used polymer membrane.
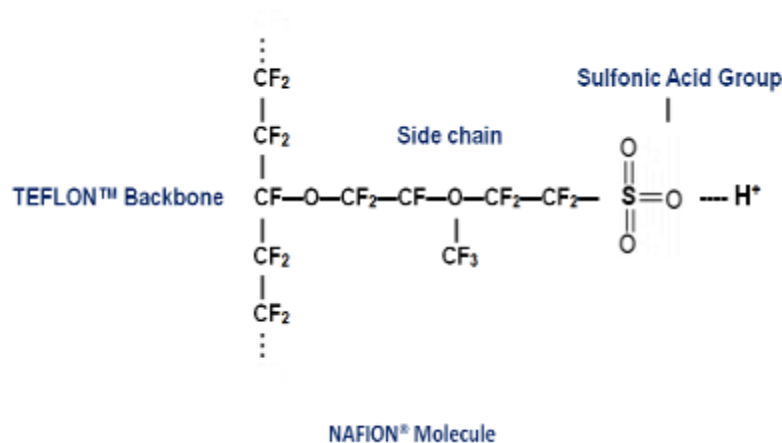
Figure 3: PTFE molecular structure (Nafion Store n.d.)

The hydrophobic main chain provides the strength for the membrane, while the hydrophilic side chains provide the proton conductivity. When the membrane becomes saturated with water, the acidic side chains dissociate into dilute acidic solutions which readily conducts protons. Protons move across the membrane under the influence of the electrical field of the MEA. These transiting protons "carry" water due to electroosmotic drag. Water can sometimes flow in the opposite direction through diffusion from the water generating cathode, resulting in an osmotic pressure gradient. Due to the clusters of hydrophilic sulfonated side chains, the membrane material can absorb large amounts of water, up to 50% by weight). Water saturation of the membrane is important because hydration promotes the transfer of H^+ ions through the membrane.

Since protonic conductivity of the membrane is heavily dependent on water content, which in turn is dependent on the structure of the membrane, it is important for a membrane to be configured in

such a way as to maximize the absorption of water. The water content in a membrane is generally expressed as the ratio:

$$\lambda = N(H_2O)/N(SO_3H)$$

where N is the number of moles. Greater concentrations of sulfonated chains results in higher water content in the membrane, thereby achieving greater proton transfer across the cell. Water uptake should be considered in the design and construction of a fuel cell because it generally causes the membrane to increase by approximately 10% in size.

With the facilitation of protonic conductivity as the primary purpose of the membrane, it is essential for the membrane to be fully hydrated. A fully hydrated solid PEM is so effective at promoting proton mobility that it is only one order of magnitude lower than an aqueous sulfuric acid solution in this metric (Barbir 2013).
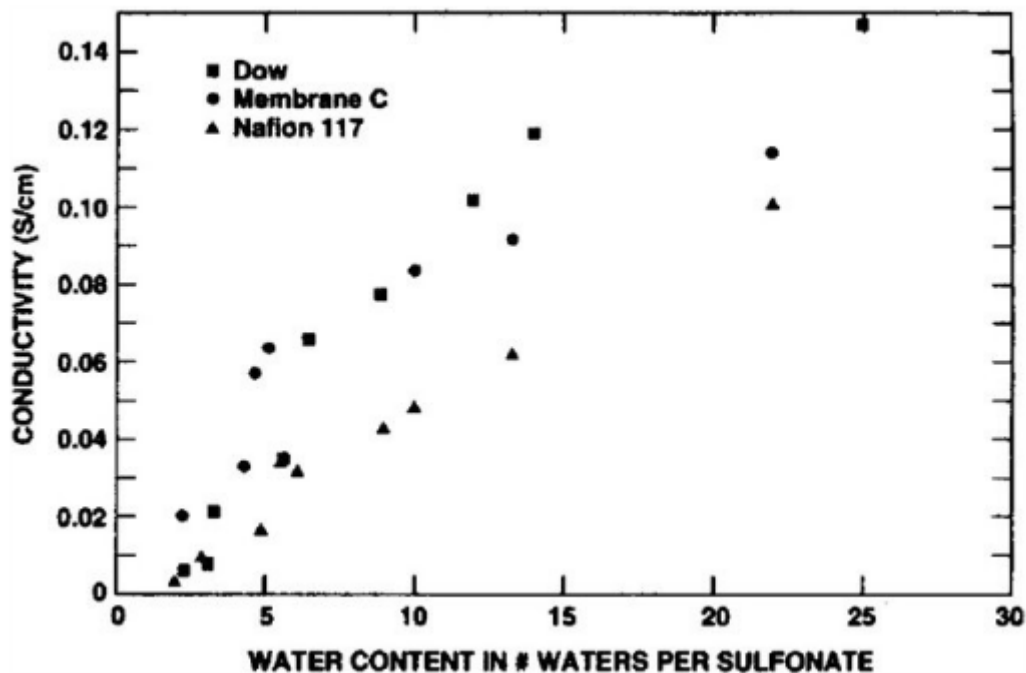
Figure 4: Relationship between proton conductivity and membrane water content (Barbir 2013)

Water Transport

Water is produced on the cathode side of the fuel cell from an oxidation reaction between H^+ and O_2, and electrons from the external current. The rate of water generation is dependent on the electrical current and is defined as:

$$N_{H2O, \, gen} = \frac{i}{2F}$$

where i is the current and F is Faraday's constant. When the current of the cell is increased, the rate of reaction increases at both electrodes, producing more water. Water also enters the cell by way of humidified gas flows. When the current of the cell increases, the gas flows increase which increases the amount of water entering the cell. As previously mentioned, electroosmotic drag causes protons moving through the electrolyte to pull water along. The amount of water carried through the membrane depends on the electroosmotic drag coefficient (ξ) of a membrane which is a function of membrane hydration (λ). This flux of water can be calculated by the equation:

$$N_{H2O, \, drag} = \xi(\lambda)\frac{i}{F}$$

Due to water production at the cathode along with electroosmotic drag, a sizeable concentration gradient can develop across the fuel cell membrane. The rate of water diffusion due to this reverse osmosis is defined as:

$$N_{H2O, \, diff} = D(\lambda)\frac{\Delta c}{\Delta z}$$

In a fuel cell using a thin membrane, the rate of water back diffusion has the potential to counteract the electroosmotic drag the results in the drying of the cell anode (Barbir 2013). This is a potential benefit of using a thin membrane in a PEMFC rather than a membrane of greater thickness that

would be impervious to water back diffusion and thus result in the drying of the anode of the fuel cell.

Electrodes

Electrodes serve the important purpose of facilitating the reactions that take place within a fuel cell to generate an electric current. Fuel cell electrodes are thin, porous layers of conductive carbon imbedded with a catalyst. The electrodes are the electrocatalytic surfaces on which the oxidation and reduction reactions occur at the anode and cathode of the cell, respectively. The need for a porous structure is for the transit of gases to and from the reaction sites on the electrode as well as the removal of water produced by the reaction at the cathode.
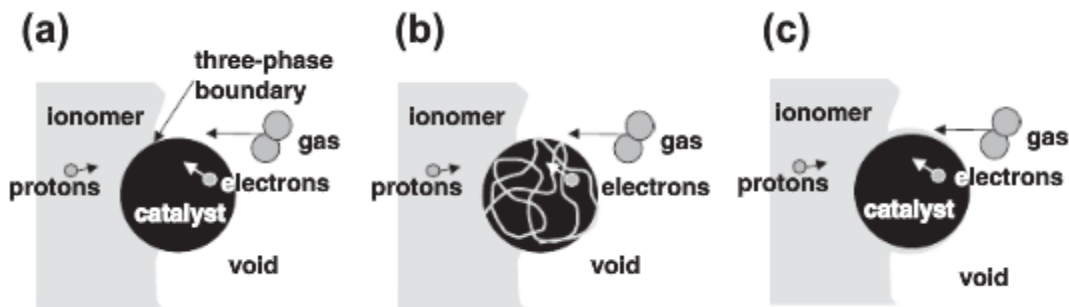
Figure 5: Representation of reaction site configurations (Barbir 2013)

In theory, the reactions occur at the electrode at the three phase boundary between the ionomer, solid, and void phases. However, due to some gas permeation through the membrane, the actual reaction zone is larger than this. It is important for the contact boundary to be increased due to the inverse proportionality between surface area and ohmic resistance. Specific manufacturing methods of electrodes address these issues with alternate ways to load the carbon ionomer with the platinum (Pt) catalyst typically used in PEM fuel cells. The use of platinum has historically been the main driver of manufacturing costs for PEMFCs. However, in recent decades, great advancements have been made to reduce the amount of platinum needed for the production of PEMFC electrodes. The

17

determining factor for reaction rate is the number of active catalyst sites which is dependent on catalyst surface area rather than the total mass. By producing a thin electrocatalyst layer with small Pt particles allows for the surface area to be maximized. Also, the combination of the membrane and catalyst layer to form a membrane electrode assembly, described previously, greatly increases cell performance. Research is being conducted to find a non-precious metal catalyst to replace platinum as a way to reduce manufacturing costs for PEMFCs (Barbir 2013).

Gas Diffusion Layer (GDL)

The layer between the catalyst layer and the bipolar plate is known as the gas diffusion layer (GDL). As its name suggests, the main purpose of a GDL is to facilitate the flow of gas from the incoming flows to the catalyst layer. GDLs also promote the removal of product water from the catalyst layer to the exiting gas flow. Gas diffusion layers also allow electrons to flow through the cell by preventing contact resistances and electrically connecting the bipolar plate and catalyst layer, completing the circuit of the fuel cell. Finally, the GDL also functions as mechanical support for the MEA and heat removal for the cell.

GDLs are generally coated with PTFE to make them hydrophobic. The weight percent of PTFE varies significantly depending on the manufacturer and intended use of the GDL. The main purpose of the PTFE is to prevent the cell membrane from flooding. It also helps to prevent water from saturating the GDL and blocking the diffusion of gas to the catalyst layer. The manufacture of the macroporous GDL with the addition of a microporous layer (MPL) can help to further reduce the likelihood of the MEA flooding. The small pores of an MPL create osmotic pressure that forces water away from the catalyst layer and out of the fuel cell. However, the degradation of the GDL and MPL has the potential to lessen this effect, thus increasing the chances of cell flooding and reduced performance. The GDL is vital to the functioning of the fuel cell by facilitating the flow of

reactants (oxygen and hydrogen) to the catalyst layer and the removal of product water from the MEA that would otherwise hinder the performance of the cell (Barbir 2013).

Bipolar Plates

Due to a single cell's relatively low voltage output, in most practical circumstances it is necessary to combine multiple fuel cells in a series, or stack. To avoid undesirable voltage drops across the stack, bipolar plates are used to connect each fuel cell. Each plate has a grooved serpentine pattern on one side to allow for gas to flow along a high percentage of the electrode surface area. Bipolar plates must conduct electricity and are therefore made of conductive materials, typically a graphite-based composite or a metallic material. The material used must be highly conductive and have low resistance to minimize voltage losses across the fuel cell. The cathode-side bipolar plate of one cell is placed in direct contact with the anode-side bipolar plate of the succeeding cell, thus facilitating a pathway of reduced electrical resistance across a battery of fuel cells (Barbir 2013).

The design of the channels on a bipolar plate should allow for the gases to reach the maximum surface area of the MEA, while also maintaining the structural support of the fuel cell. Sharp corners in the flow pattern on a bipolar plate leads to greater pressure drop, which is detrimental to cell performance. A thinner bipolar plate translates to decreased electrical resistance, but also less structural stability and tighter channels for gas flow (Larminie and Dicks 2003).

Fuel Cell Testing Techniques

To determine the effect of GDL degradation on fuel cell performance, characterization tests were performed on the fuel cells to determine base level performance and how that performance changed as the degradation testing progressed. The characterization testing comprised of electrochemical

tests that are detailed in this section below. Physical tests were also performed on GDLs using a scanning electron microscope (SEM).

Chronoamperometry (CA)

Chronoamperometry is an electrochemical method where a constant voltage potential is applied to, in this case, a fuel cell. The resulting data is displayed as a plot of current vs. time. By performing CA testing at multiple fixed potentials, the resulting data can be combined to create a polarization curve that represents the relationship between current and potential across a wide spectrum of potentials. This gives a researcher a general view of the performance of the cell and by comparing the polarization curves (voltage vs. current) from different points in the experiment, changes in fuel cell performance can be discerned.

Due to the proportional inverse relationship between current and potential (potential decreases proportionally to increases in current and vice versa), the performance of a fuel cell can generally be ascertained from the slope of the polarization curve. Another insight that a polarization curve using CA data can give on how a fuel cell is performing is at the part of the polarization curve that depicts the relationship between current and potential at very low voltage potentials. It is generally the case that below a certain potential, the current of the cell is high enough to drive the reduction of oxygen at the cathode at a rate greater than the cell's air supply rate. This causes the current of a fuel cell to level out at very low potentials due to the limitations of the fuel cell in terms of the amount of current it can supply to the system (Rao and Rengaswamy 2006).

Chronopotentiometry (CP)

Chronopotentiometry is the most basic constant current experiment. As that brief description suggests, CP works by applying a constant current to the cell and reading the resulting voltage as a

function of time. The potential vs. time curve is determined by the concentration profiles of the redox species as a function of time. At OCV, when no current is being applied to the cell, the concentration of O_2 at the cathode surface is equivalent to its concentration in the bulk airflow. The initial potential of the cell in this resting state is known as OCV and is the maximum potential that the cell can produce on its own. When the steady current is applied to the cell, the O_2 at the cathode surface is reduced to O_2^{2-} in order to support and maintain the applied current. As this redox reaction occurs at the cathode, the concentration of O_2 at the electrode surface decreases. The potential of the cell at a certain current is tied to the redox potential of ½ O_2 + 2 e^- → ½ O_2^{2-} and depends on the Nernst Equation:

$$E = E^{\circ`} + \frac{0.059}{n} log \frac{C_o}{C_x}$$

where C_o and C_x represent the concentrations of O_2 and O_2^{2-} at the cathode surface, respectively (Chronopotentiometry n.d.) (Bott n.d.).

By performing CP tests on a fuel cell at a range of currents, the data can be compiled to form a polarization curve. A polarization curve shows the relationship between current and voltage for a cell by overlaying slopes of current vs. time and voltage vs. time. Polarization curves for a fuel cell performed at different points during the experiment are compared to determine any change in fuel cell performance. Degradation of the fuel cell would be indicated by a decrease in the voltage potential produced over the course of the experiment when holding current constant.
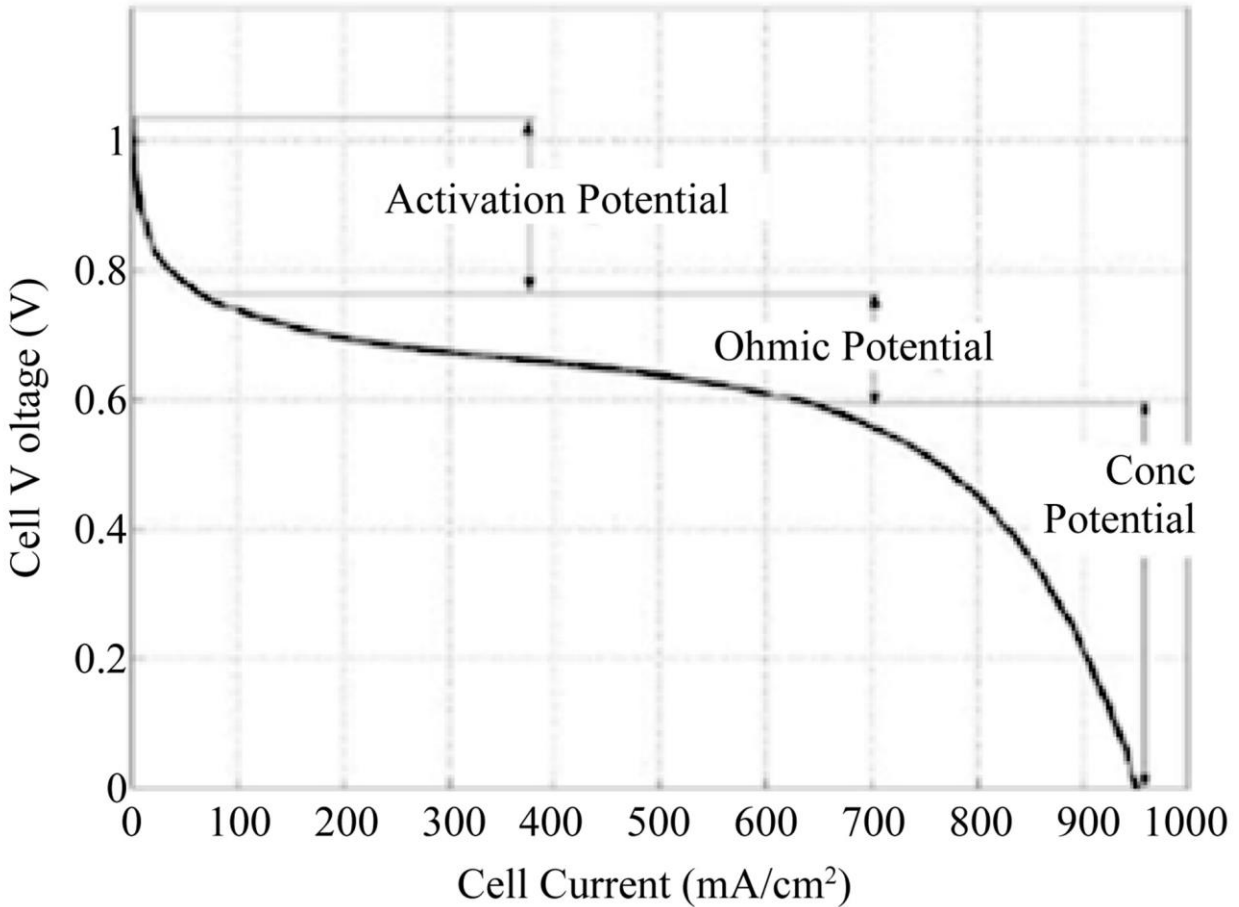
Figure 6: Typical Polarization Curve (Cultura and Salameh 2014)

Cyclic Voltammetry (CV)

Cyclic voltammetry is an in situ electrochemical testing technique used to measure the electrochemical surface area (ECA) of a gas diffusion electrode. CV works by subjecting the cell to a potential that oscillates back and forth between two voltage limits while the resulting current is recorded. The data is displayed as a plot of current vs. voltage and is known as a cyclic voltammogram. When a CV test is performed on a fuel cell, hydrogen is fed to the anode while an inert gas, usually nitrogen, is fed to the cathode in place of the typical operating feed of air or oxygen.

The peaks on the left side of a cyclic voltammogram are the main reason for running this test. These peaks are caused by hydrogen adsorption and desorption reactions on the platinum catalyst in the cell. The adsorption/desorption charge can be calculated by determining the area underneath the peaks of interest. From this value, the ECA of the working electrode in the fuel cell can be determined using the following equation:

$$ECA(cm^2 \, Pt/gPt) = \frac{Charge(\mu C/cm^2)}{210\left(\frac{\mu C}{cm^2 Pt}\right) \times Catalyst \; Loading(gPt/cm^2)}$$

Something to note about this test is that, for a fuel cell using a carbon-supported electrocatalyst, the presence of carbon can alter the hydrogen adsorption and desorption characteristics (Barbir 2013).

Electrochemical Impedance Spectroscopy (EIS)
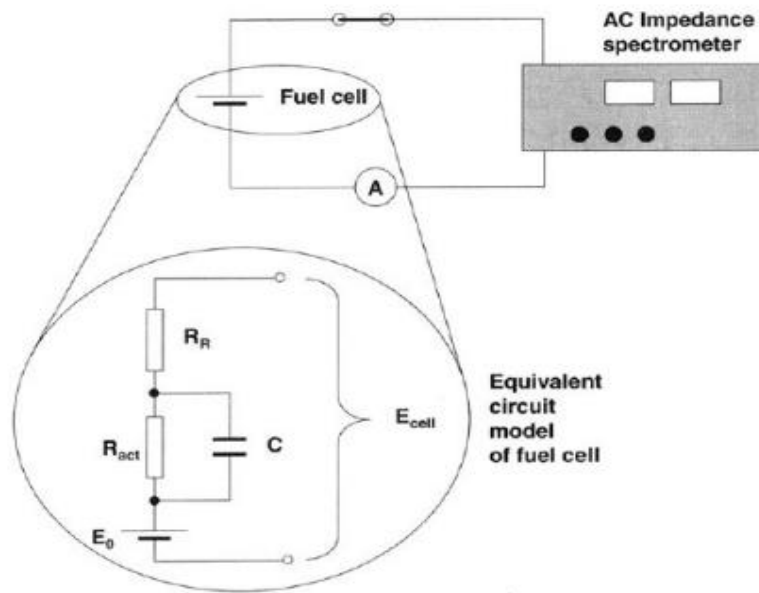
Figure 7: Fuel cell circuit for EIS (Barbir 2013)

EIS works by applying a small ac voltage or current perturbation/signal to the cell and measuring the resulting signal's amplitude and phase as a function of frequency (Wu, et al. 2008). This test is generally performed at a wide range of frequencies and is used to determine the impedance to

current of a fuel cell. The impedance measured by EIS is due to double layer capacitance, charge

transfer resistance, ohmic resistance, and mass transport limitations.
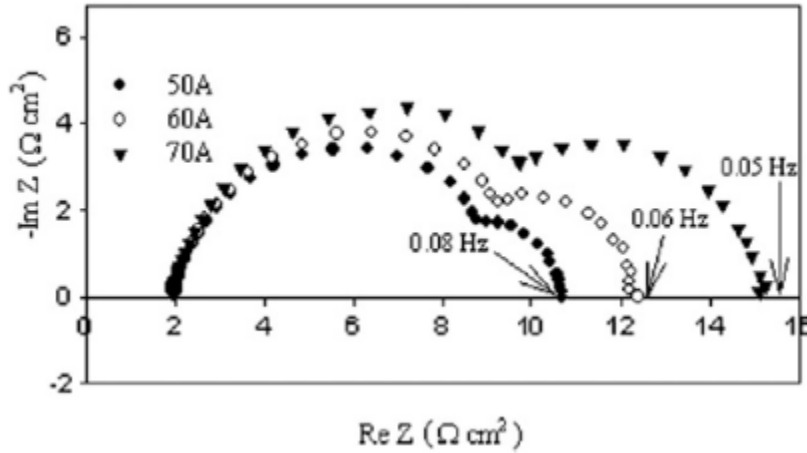
Figure 8: Typical impedance spectra for PEMFC (Barbir 2013)

EIS data are typically presented by a Nyquist plot characterized by two arcs. The high frequency arc

reflects the impedance caused by charge transfer resistance, the intersection of the high frequency

arc and the x-axis determines ohmic resistance, and the low frequency arc reflects impedance in the

system caused by mass transport limitations. Performing EIS at a range of currents gives insight into

the limiting factors of fuel cell performance and how it is affected by the operating electrical current

(Barbir 2013).

Linear Sweep Voltammetry (LSV)

LSV is used to determine the rate at which hydrogen and oxygen permeates the cell membrane. As

mentioned before, the main purpose of the membrane in a PEMFC is to facilitate the movement of

hydrogen protons from the anode to the cathode while preventing the transfer of diatomic hydrogen

and oxygen molecules, along with electrons, across the cell. Therefore, any gas crossover diminishes

the fuel cell's performance and is undesirable.

Like CV tests, hydrogen is supplied to the anode and an inert gas, usually nitrogen, is supplied to the cathode in place of oxygen/air. A linear voltage is applied across the cell and the current is measured and plotted against voltage. Because only inert gas is fed to the cathode, the entirety of the electrical current measured is due to the electrochemical oxidation of hydrogen gas, at the cathode, that permeated the membrane. A higher current signifies a higher rate of gas crossover in the cell. Gas crossover increases with voltage and reaches a limiting point at around 400 mV, at which point any hydrogen gas crossing over is instantly oxidized due to the overpotential. Based on the determined limiting current of the cell, the hydrogen gas crossover flux can be calculated using Faraday's Law:

$$m = (\frac{Q}{F})(\frac{M}{z})$$

The current produced by gas crossover is a good indicator of the physical state of the fuel cell membrane. By performing LSV tests before and after degradation trials, it is possible to see what effect different simulated exposures have on the structural stability of fuel cell membranes (Barbir 2013).

Scanning Electron Microscope (SEM)

A scanning electron microscope is a microscope that uses a focused beam of electrons to produce small-scale images of a sample. The feedback from how the electrons interacted with the sample is used to create an image of the sample surface. We used an SEM to provide visual evidence of physical degradation of the GDLs that were subjected to degradation tests.

Potential Applications

The future of fuel cells remains uncertain. The technology holds promise for an efficient, reliable, and environmentally conscious energy source. However, there are still many technological hurdles, previously mentioned in this paper, which will need to be overcome before fuel cells become a viable replacement for existing energy technology.

PEM fuel cells, in particular, have potential automotive applications. Due to their light, compact design and low operating temperature, vehicles powered by PEMFCs could account for a share of the cars on the road by replacing existing combustion engines and battery-powered electric vehicles (EVs). While a combustion engine's maximum efficiency is at or near its maximum power output, a fuel cell's maximum efficiency is generally at a partial load which tends to be the most common power supply state during vehicle operation (Barbir 2013). What our research, and the research of many other scientists, has worked to solve is the lack of reliability and durability that currently constrains fuel cell viability as a vehicular power generator. With the present high rates of carbon degradation, PEMFCs are not economically viable options to replace battery-powered EVs, let alone traditional combustion engine cars.

Previous research indicates that much of the fuel cell degradation is caused by inconsistent power demands on the fuel cell. When the voltage of a cell changes rapidly, or the cell is run outside the range of 0.2-0.6 V, the rate of degradation typically increases dramatically. A solution to this problem is currently being tested at LRGP. The experiments center on the introduction of supercapacitors to the fuel cell system. The hypothesis is that, as the power demand on the fuel cell changes suddenly, the supercapacitor tempers the rate at which the fuel cell needs to adjust its current. When the fuel cell is producing more current than is demanded by the system, the supercapacitor absorbs the excess current, thereby charging itself. Inversely, when the system

suddenly demands a greater current than the fuel cell is currently producing, the supercapacitor

discharges its stored power, allowing the fuel cell to step up its power output more gradually. This is

intended to reduce the overall wear on the cell and, in theory, minimize the rate of degradation. It

remains to be seen whether the addition of supercapacitors, or other advancements, will transform

fuel cell technology into an economically viable and commercially available power source for

automobiles. However, the continued dedication and innovation of leading researchers in the field

are constantly pushing the boundaries of fuel cell technology and may yet overcome the remaining

hurdles the promising technology of fuel cells faces.
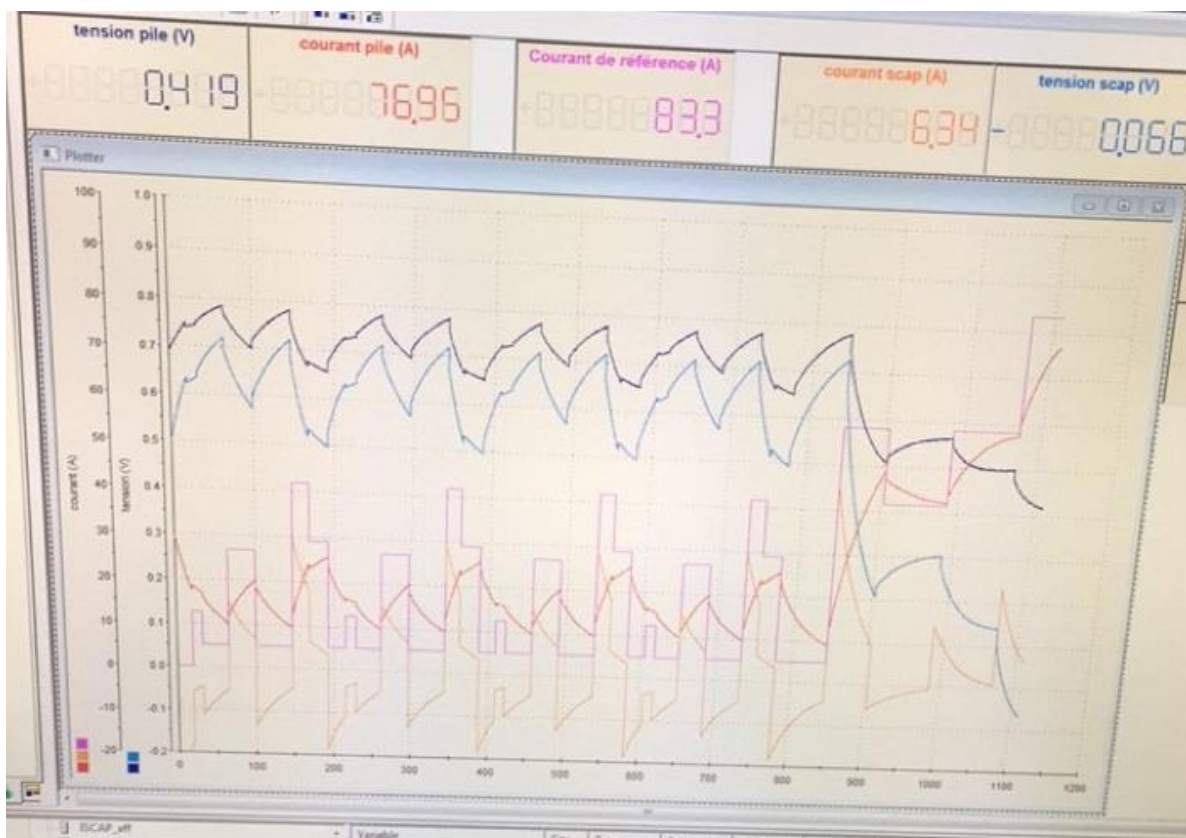
Figure 9: Cycling of Fuel Cell Supported by Supercapacitor

Solving the technological challenges of fuel cell operation is only one side of the coin, however.

Generating the fuel that fuel cells require is potentially of greater importance in terms of

environmental concerns. While fuel cell technology does offer the potential of higher efficiency than

combustion engines and only produces water as a direct product, if the source of the hydrogen consumed by the fuel cell is still sourced from hydrocarbons then the reduction in carbon emissions won't be nearly as significant. The use of hydrogen is beneficial due to the higher heating value of hydrogen compared to gasoline. In fact, the amount of energy in 1 g of hydrogen is equivalent to the energy of 2.73 g of gasoline (Barbir 2013). Advancements in water hydrolysis technology could address this issue and allow for the creation of a closed-loop water hydrolysis/fuel cell (reverse hydrolysis) system. The field of fuel cell technology holds both great promise and great challenges.

Methodology

Equipment

Large Fuel Cell

The large fuel cell housed a MEA of 100 cm^2 (10cm · 10 cm). The PEM was a Nafion™ 115 membrane fabricated by DuPont, the electrodes were made by PaxiTech, and the GDL was produced by an associated private lab. The electrode had 0.5 mg of platinum per cm^2, a ratio of 40% Pt to carbon, and consisted of a non-woven GDL with microporous layer. The GDL used was designed after Sigracet® 24BC series GDL, which has a thickness of 235 μm (9.3mil), an areal weight of 100 g/m^2, air permeability of 0.6 $cm^3/(cm^2 \cdot s)$, and an electrical resistance through the plane less than 12 $m\Omega cm^2$. The MEA was constructed by the same associated lab, located in Grenoble, France, responsible for fabricating the GDL. The large fuel cell housing contained the complete requirements for fuel cell operation, including bipolar plates with channels for gas distribution, current collecting plates, and cooling/heating water channels in the end plates. Figure

XXX shows the design of the Fuel Cell, including MEA, bipolar plate, current collecting plate, end plates, as well as the inlets and outlets of the fuel cell.

Large Fuel Cell Bench

The large fuel cell was placed into a fume hood which contained the necessary gas lines, pressure apparatus and preparatory feed equipment. Air and hydrogen entered from the house feed. Brooks® mass flow regulators controlled both air and hydrogen lines. Each line then entered a humidifier which was maintained at 60℃, and then traveled to the fuel cell. The humidified lines to the fuel cell were wrapped in heating coils and insulation set to maintain the temperature of 60℃. After passing through the fuel cell, the gas lines passed an electro vane system designed to operate the fuel cell at 1.5 bar. The fume hood also contained a pressure regulator control box connected to sensors in the feed and exit lines, as well as the electro vanes to control the pressure. Water heaters for both the fuel cell and humidifiers were located outside of the fume hood and maintained the set temperatures (80℃ and 60℃ respectively). There was also an additional small peristaltic pump to maintain the water levels in the humidifiers for extended periods when the lab was closed. The large fuel cell was also connected to a Kikusui Electronic Load PLX664WA, which was controlled by a computer running dSpace ControlDesk 3.7.5. The dSpace ControlDesk ran programs developed by LRGP to perform cycling and polarization curve tests. Additionally, dSpace ControlDesk software controlled the Brooks® mass flow regulators, adjusting the flows based on Faraday's Law and the set stoichiometric ratio. In order to accomplish additional tests, the fuel cell was connected to BioLogic 80Amp Booster (VMP3B-80), which was controlled by a BioLogic VSP potentiostat. The BioLogic apparatus was controlled by EC-Lab software.

Small Fuel Cell

The small fuel cell housed a 7.5 cm^2 MEA (2.5 cm · 3 cm). The PEM was a Nafion™ 115 membrane fabricated by DuPont, the electrodes were made by PaxiTech, and the GDL was produced by Sigracet®. The electrode had 0.5 mg of platinum per cm^2, a ratio of 40% Pt to Carbon, and consisted of a non-woven GDL with microporous layer. The GDL utilized was Sigracet® 24BC series GDL, which has a thickness of 235 μm (9.3mil), an areal weight of 100 g/m^2, air permeability of 0.6 cm^3/(cm^2· s), and an electrical resistance through the plane less than 12 mΩcm^2. Alternative tests were accomplished with Sigracet® 24BA series GDL, which has a thickness of 190 μm (7.5mil), an areal weight of 54 g/m^2, air permeability of 60 cm^3/(cm^2· s), and an electrical resistance through the plane less than 10 mΩcm^2. The MEA was constructed in-house using electrodes sized to 2.5 cm · 3 cm, GDLs sized to 2.5 cm · 3 cm, PEM sized to 4.5 cm · 4.5 cm, and a titanium mesh sized to 4 cm · 4 cm. The titanium mesh was used to separate the electrode and GDL on the cathode side in order to enable separation and analysis of the GDL. The small fuel cell housing contained insulating plates, current collector plates, bipolar plates, and end plates. The bipolar plates had an access point for a thermocouple and the end plates had slots for heating rods.

Small Fuel Cell Bench

The small fuel cell was placed on an open air bench with necessary gas lines. The feed lines went through Brooks® mass flow regulators controlled by a Brooks® 0254 Batch/Blend Control Display. The air feed line then went to a humidifier which was at ambient temperature, the humidified line to the fuel cell was heated by heating coils and insulated, the heating coils were set to 38℃. The hydrogen feed went directly to the fuel cell without humidification or heating. The bench also had a heating unit utilizing a thermocouple placed in the bipolar plate and heating rods placed in the end plates, the temperature for the fuel cell was set at 42℃. The fuel cell was connected to BioLogic 80Amp Booster (VMP3B-80), which was controlled by a BioLogic VSP potentiostat. The

BioLogic apparatus was controlled by EC-Lab software. The flows were manually imputed using the Brooks® 0254 Batch/Blend display.

Characterization Equipment

The large fuel cell was connected to a Kikusui Electronic Load PLX664WA, which was controlled by a computer running dSpace ControlDesk 3.7.5. The dSpace ControlDesk ran programs developed by LRGP to perform cycling and polarization curve tests; additionally, dSpace ControlDesk software controlled the Brooks® mass flow regulators, adjusting the flows based on current applied load. In order to accomplish additional tests, the large fuel cell was connected to BioLogic 80Amp Booster (VMP3B-80), which was controlled by a BioLogic VSP potentiostat. The BioLogic apparatus was controlled by EC-Lab software.

The small fuel cell was connected to BioLogic 80Amp Booster (VMP3B-80), which was controlled by a BioLogic VSP potentiostat. The BioLogic apparatus was controlled by EC-Lab software. The flows were manually imputed using the Brooks® 0254 Batch/Blend display.

Ex Situ Aging Apparatus

Two ex Situ aging tests were performed: 1) electrochemical corrosion in an acid bath, and 2) acid bath purged with air.

Electrochemical Corrosion in Acid

The GDL sample was placed in a 0.5M solution of H_2SO_4, with an opposite electrode, and a reference electrode. The container was placed in water bath set to 60℃. Figure 10 shows a schematic illustration. The temperature was controlled by a Fischer Scientific Isotemp® hot plate and magnetic stirrer.
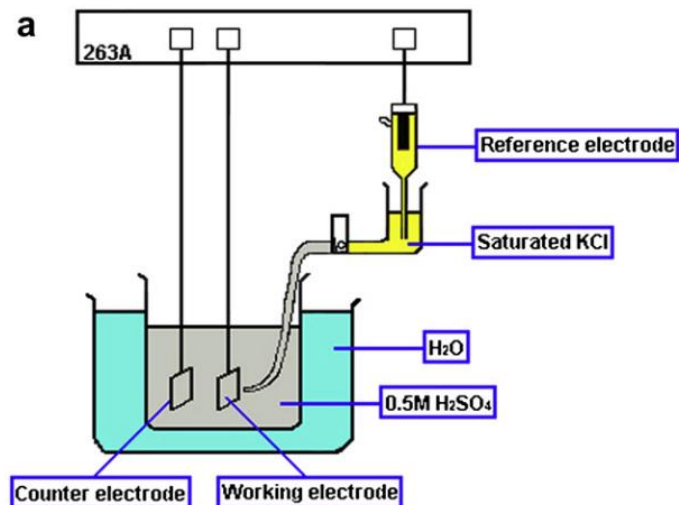
Figure 10: Three-electrode cell setup for corrosion test (Chen, et al. 2009)

Acid Bath with Air Purge

GDL samples were placed in a beaker with a 1M solution of H_2SO_4 was maintained at 60℃, with an air purge. The air purge is provided through a porous glass tube. The temperature was controlled by a compatible control CC3 recirculating water heater. Figure 11 is a picture of the beaker and air purge setup.
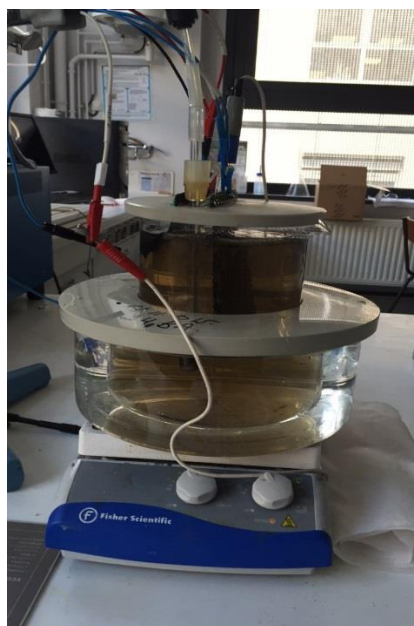
Figure 11: Acid Bath w/ Air Purge Setup

Procedures

Cycling

The fuel cell was set to run at 80°C, 50% RH, and stoichiometric coefficients of 1.2 and 2.0 for hydrogen and oxygen, respectively. The fuel cell was operated under pressure, with incoming air and hydrogen flows regulated at 1.500 bar. Conditioning was performed for 15 hours to allow the new membrane to mature. Characterization tests were then performed to determine the cell's base state. Electrochemical tests performed include chronopotentiometry (CP), electrochemical impedance spectroscopy (EIS), cyclic voltammetry (CV), and linear sweep voltammetry (LSV). LSV and CV are performed in humid cell conditions only, while CP and EIS are performed in humid, operating, and dry cell conditions. These different humidity conditions were achieved by adjusting the temperature of the cell. Once all the data for the fuel cell's initial performance is collected, the cell was put through a cycling process for four days (100 hours), with each cycle lasting 20 minutes. The cycling is based on the New European Degradation Cycle (NEDC), which is a simulation of a real internal engine vehicle working under idle running, constant load running, variable load acceleration, full power running and overload running conditions. At the completion of the four-day cycle, another round of characterization testing was performed to determine the effects of cycling on the fuel cell's performance. This procedure was repeated for a full month (500 hours).

Ex-Situ Aging

Electrochemical Degradation

An acid bath of 0.5 M H_2SO_4 was prepared and deposited into a large beaker. A 24BC GDL was hung in the solution, along with a titanium mesh, a porous glass tube distributing nitrogen

throughout the solution, and a reference electrode. A voltage of 1.2 V was applied to the system. The GDL remained in the acid bath for four days, with a sample of the GDL taken every 24 hours. The GDL samples were tested with a SEM to determine the physical effects of a large voltage potential and the presence of acid. This process was repeated with potentials of 1.0 V and 1.4 V. IR testing of samples of the acid solution, taken at 24-hour intervals, was inconclusive.

Immersion

A beaker of 1.0 M H_2SO_4 was prepared and multiple pieces of 24BC GDL were immersed. The beaker was then placed in a vacuum for four days. Upon removal from the vacuum, the pieces of GDL were immersed in a 1.0 M H_2SO_4 acid bath. A porous glass tube was inserted into the bath to deliver air. Every 24 hours a sample was removed from the bath and placed in the oven to dry for 24 hours. These pieces were tested using a SEM to view any physical degradation caused by immersion in acid.

In-Situ Aging

Carbon Corrosion

A smaller fuel cell was used to test the difference in carbon corrosion of GDLs with microporous layers (MPL) and those without. GDLs with a MPL are referred to as 24BC while those without a MPL are referred to as 24BA. The testing began with the construction of fuel cells with each type of GDL. Each cell was conditioned for two days and subsequently characterized by performing CP and EIS. Two more cells were made, one with 24BA and the other with 24BC, with the inclusion of a layer of titanium mesh. The previous two cells contained an extra gasket to nullify the potential effect of cell thickness on fuel cell performance. The two cells containing the titanium

mesh were put through the same conditioning and characterization process. The results of the four cells were then compared to determine the effects, if any, of the MPL and titanium mesh on base fuel cell performance. Once determined, a cell constructed using 24BA and titanium mesh was run at 1.2 V for four days, after initial conditioning and characterization. After the four days, another round of CP and EIS was performed and the data were compared to data collected from the initial characterization to determine the effect of a large sustained voltage potential on fuel cell performance. The same process was also performed for a fuel cell using 24BC in place of 24BA.

Characterization

Characterization differed for the two benches. For the large fuel cell characterization included several polarization curves (based on a modified chronopotentiometry), EIS, CV and LSV. These tests were performed every 100 hours of cycling for a total of 500 hours. The tests began with a polarization curve at operating conditions, then EIS was performed at 10, 30, 50, 70, and 80 amps. The temperature of the fuel cell was then reduced to 60℃ to reach humid conditions. After reaching steady state, the polarization curve was performed again. After this the air feed line was replaced with a nitrogen feed. After purging all air and oxygen from the system, denoted by a drop in cell voltage, CV and LSV were performed. Afterward the air was replaced, the temperature of the cell increased to operating conditions at 80℃. When steady state was achieved, another polarization curve was performed. Then the cell was tested at dry conditions, and the humidifier temperature was dropped to 43℃. When the cell reached steady state at the dry conditions, a final polarization curve was performed. The polarization curves were performed by the Kikusui Electronic Load PLX664WA. The polarization curve program was executed by dSpace ControlDesk 3.7.5. The dSpace ControlDesk controlled both the applied current and the flow rates of air and hydrogen. The program was executed to three conditions: 1) test must take 30 minutes, 2) test from 0-130 amps, 3)

current was stepped by a) 0.5A for less than 10A, and b) 1A for current greater than 10A. Each step of current was performed for 13 seconds. For EIS, CV, and LSV tests, the fuel cell was connected to a BioLogic 80Amp Booster (VMP3B-80), which boosted a BioLogic VSP potentiostat. The BioLogic apparatus was controlled by EC-Lab software.

Characterization tests for the small fuel cell were performed by a BioLogic 80Amp Booster (VMP3B-80), which boosts a BioLogic VSP potentiostat controlled by EC-Lab software. Chronopotentiometry (CP) was performed at set currents, the average potential or voltage was read and a polarization curve was produced. EIS was also performed at each current as well. The tests were performed sequentially in EC-Lab; CP for 10 minutes, followed by EIS. After the tests were done, the flows were adjusted for the next current and the tests were performed again.

Results

Cycling

The Membrane Electrode Assembly (MEA) provided by CEA-Grenoble was compared to commercially available MEA manufactured by Solvicore. The cycling and characterization of the Solvicore sample was completed before January 2016. The voltage response of the Solvicore sample is provided in Figure 12, showing performance after conditioning and after 500 hours of cycling.
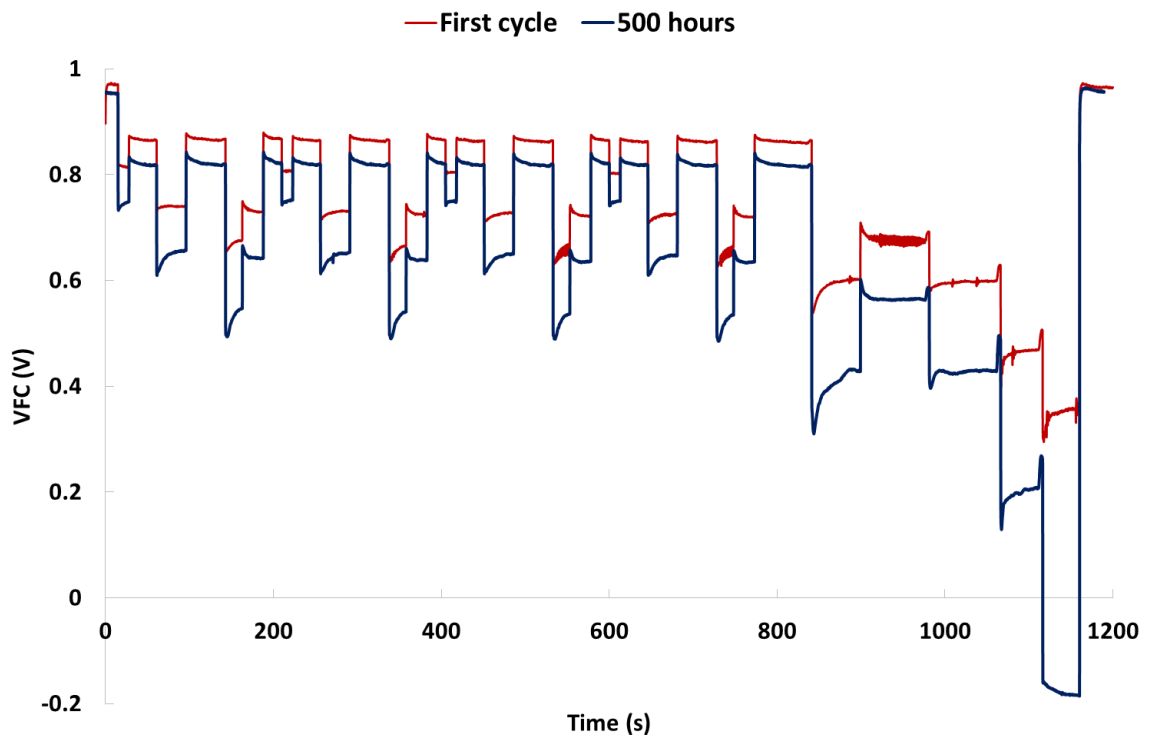
Figure 12: Solvicore New European Driving Cycle Results

The results here show typical degradation of the fuel cell after accelerated stress tests. With drastic failure of the cell at higher currents, the Solvicore MEA drops into negative voltage, performing electrolysis of water instead of the reverse reaction. However, other standards of the fuel

cell remain constant, Open circuit voltage is constant at ~0.95 volts. Other characterization tests reveal that all aspects of the MEA continued to function after 500 hours, revealing that the point of failure was the gas diffusion layer. For more detailed analysis of the fuel cell performance, please reference sections "Polarization Curves" through "Cyclic Voltammetry" in the Results section for each characterization test.

The MEA from CEA-Grenoble was cycled through the same accelerated stress test, the New European Driving Cycle. The results for the CEA-Grenoble MEA is shown in Figure 13. The first noticeable result is the improved performance at higher currents, the second anomaly is the drop in the open circuit voltage. Over the course of the 500 hour of cycling, the open circuit voltage dropped from 0.99 V to 0.82 V. This result can be attributed to the formation of holes in the membrane as revealed by LSV, and is explained in more detail in a later section, labeled "Linear Sweep Voltammetry."
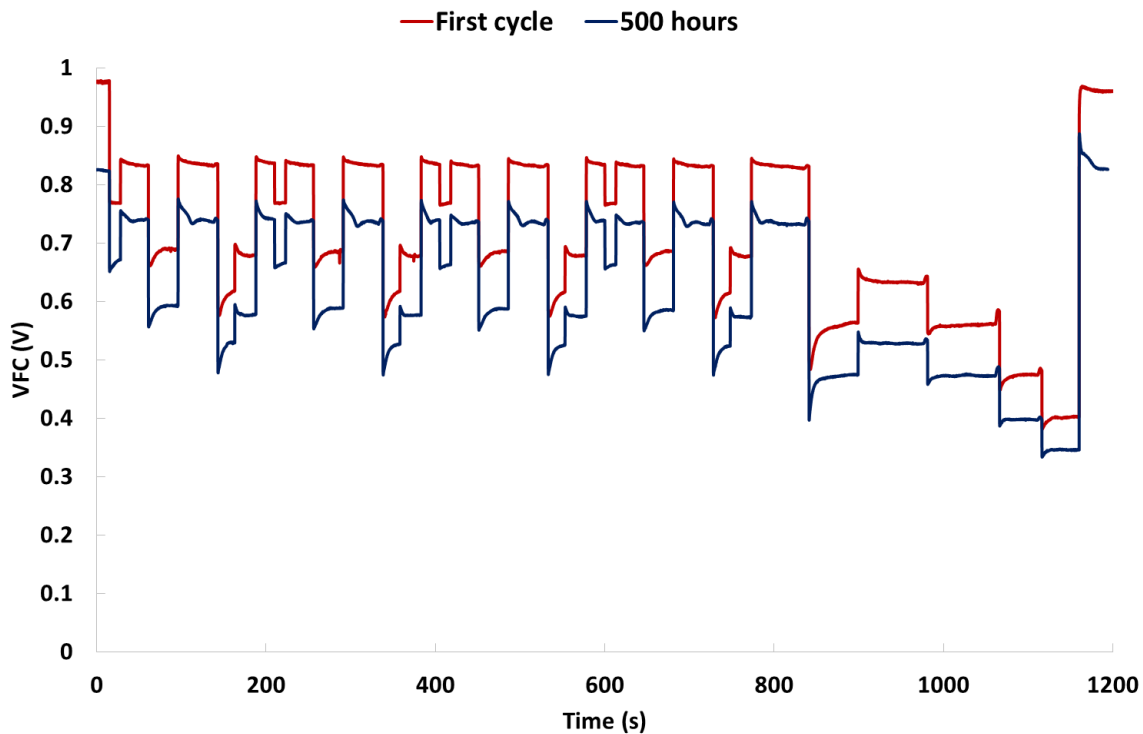
Figure 13: CEA-Grenoble New England Driving Cycle Results

Polarization Curves

The polarization curves show the voltage across the cell for each current drawn from the cell, and provides a "snapshot" of fuel cell performance. A polarization curve also indicates the general areas of fuel cell failure. The curve can be divided into three areas, the first section, at low current, represents activation losses. A sharp drop in voltage is present and represents irrecoverable losses. At medium current the voltage drop is linear, and is a direct result of the ohmic resistance of the fuel cell. And finally at high current, the voltage drop becomes quite large. This final section is known as the mass transfer resistance. It is caused by a large amount of water is created at the cathode under high current. This water surrounds the catalyst particles, creating a barrier for oxygen particles to diffuse through in order to complete the reaction. This extra barrier reduces the voltage output of the cell.

The polarization curves of both the MEA provided by CEA-Grenoble and Solvicore are shown below in Figure 14.
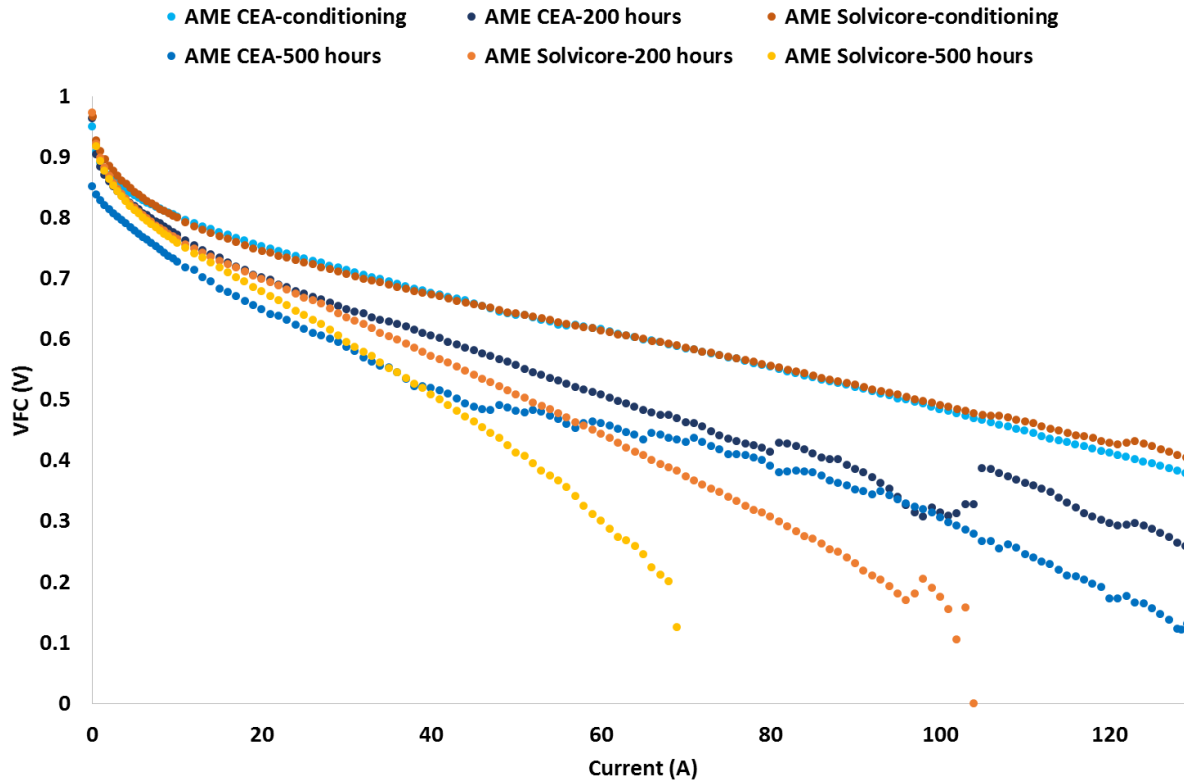
Figure 14: Cycling Polarization Curves

It is readily apparent that the MEA from CEA-Grenoble provides must better performance throughout the range of currents tested. While both MEAs provided almost identical performance after conditioning, the Solvicore MEA deteriorated rapidly. Another way of viewing the polarization curve is provided in Figure 15, which shows the degradation of voltage at set currents as a function of cycles performed on the cell.

The voltage jumps seen around the 100 A mark indicate the back-diffusion of water across the membrane from the cathode to the anode. As water is produced at the cathode and water crosses the membrane from the anode to the cathode due to electro-osmosis, a water gradient forms. When the gradient reaches a certain level, back-diffusion occurs. The jump in voltage observed in our research supports previous findings by other researchers that the water distribution

in the MEA is dependent on current density (Song, et al. 2008). It was only at high current density that back-diffusion was observed in the cell.
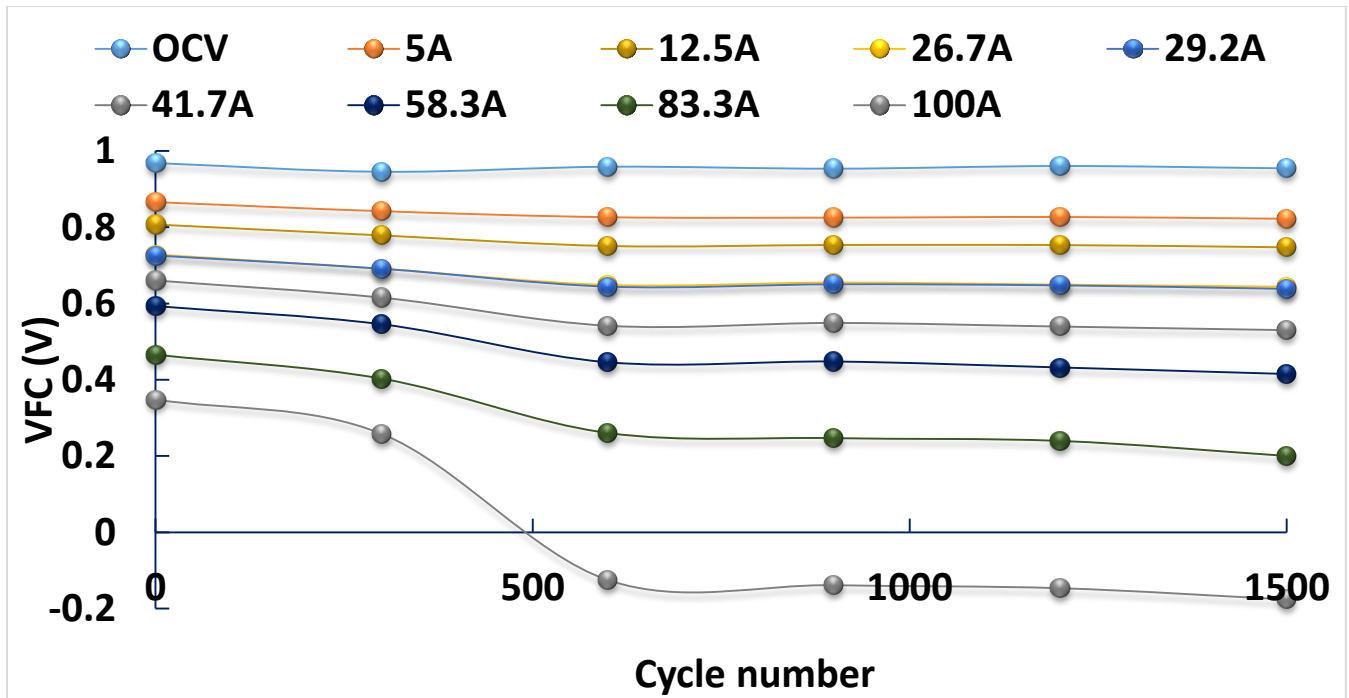
Figure 15: Solvicore Performance per Cycle

From this graph it is obvious to see that the majority of the degradation occurred after 300 cycles and before 600 hours, or 100 and 200 hours of cycling. The major drop in performance is also at 100A, the highest current tested. This is an indication of the failure of the gas diffusion layer to remove sufficient water from the MEA catalyst layer, resulting in decreased performance. The slope of the second "region" of the polarization curve also indicates that there is increased ohmic resistance in the Solvicore MEA. These aspects are investigated more thoroughly in the upcoming sections.

The CEA-Grenoble MEA exhibited more consistent performance for throughout the cycling tests, as shown in Figure 16.
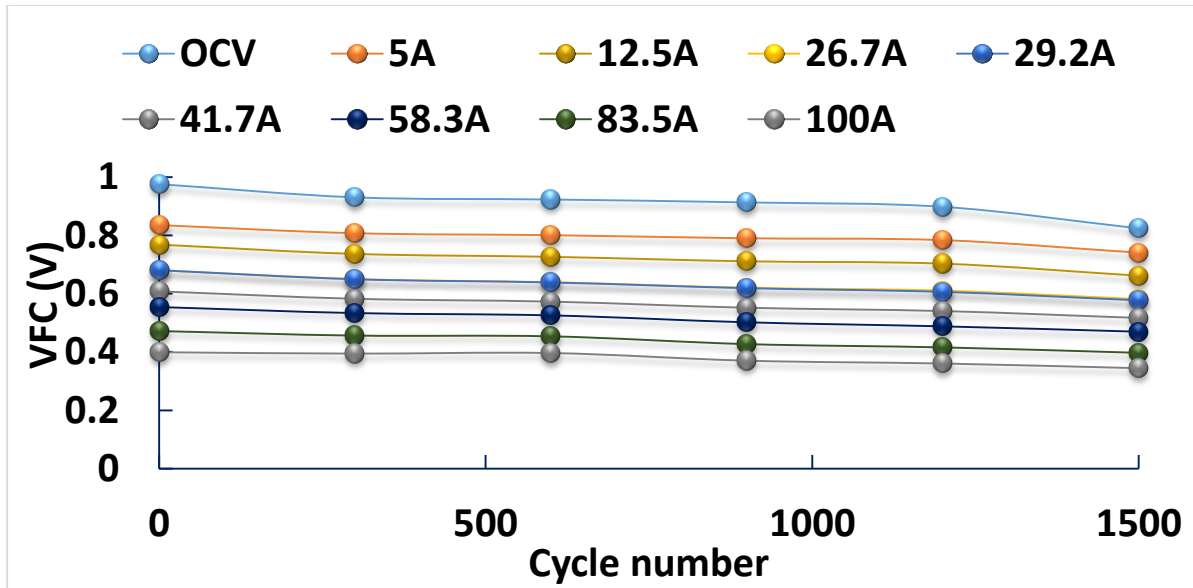
Figure 16: CEA-Grenoble Voltage Performance per Cycle

The polarization curves indicated that the major barriers to fuel cell performance lie in the

The major losses for the CEA-Grenoble MEA happen at the opposite end of the current spectrum.

At open circuit voltage (OCV), the voltage drops are related to the crossover of hydrogen molecules.

This crossover of Hydrogen molecules is related to holes in the polymer electrolyte membrane. The

performance of the fuel cell at other currents indicate reduced ohmic losses and improved water

management at higher currents.

The CEA-Grenoble MEA shows that drastically improved fuel cell performance can be achieved

through modifications of the gas diffusion layer. Fuel cell performance is improved at moderate

currents through reduced ohmic resistance and improved water management improves performance

at higher currents.

GEIS

Galvano Electrochemical Impedance Spectroscopy reveals specific factors of fuel cell

performance. EIS data can be analyzed qualitatively from the graphs below, and then fitted through

excel in order to quantitatively assess the different performance of the different MEAs. EIS data

provides the anode and cathode charge transfer resistance or activation losses, the ohmic resistance

as well as the diffusion resistance. EIS also detects the pseudo capacitance of the cell, but this value

is not of interest to the degradation of the GDL. The overall EIS spectra can be analyzed via the

following graphic.
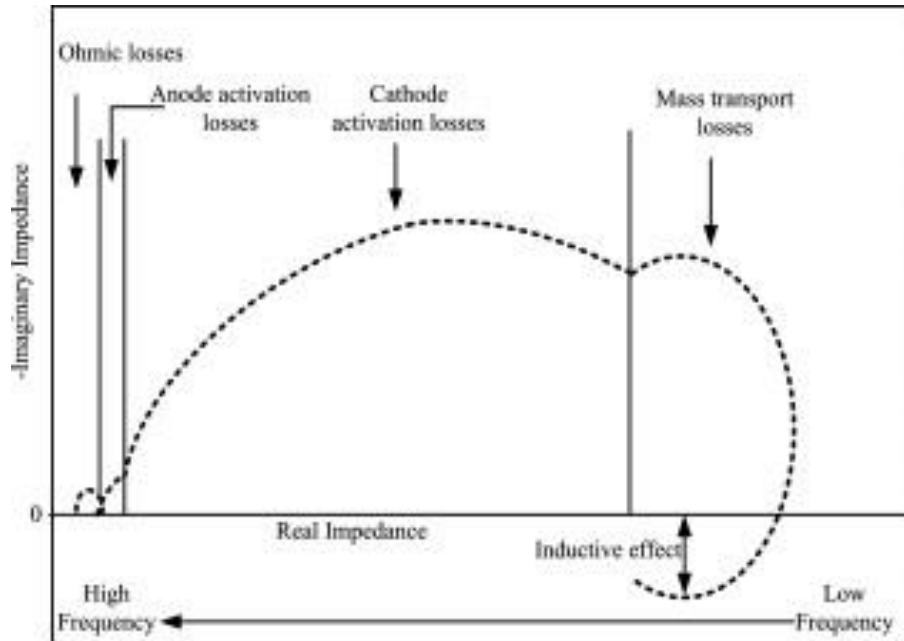
Figure 17: EIS Example (Dale, et al. 2010)

For PEM fuel cells, the anodic activation losses are small compared to the cathode resistance

to charge transfer and can be neglected. By analyzing the respective areas of each region, the specific

losses for each area of the fuel cell can be accurately assessed.

The EIS spectra for the Solvicore MEA is shown in Figure 18, below.
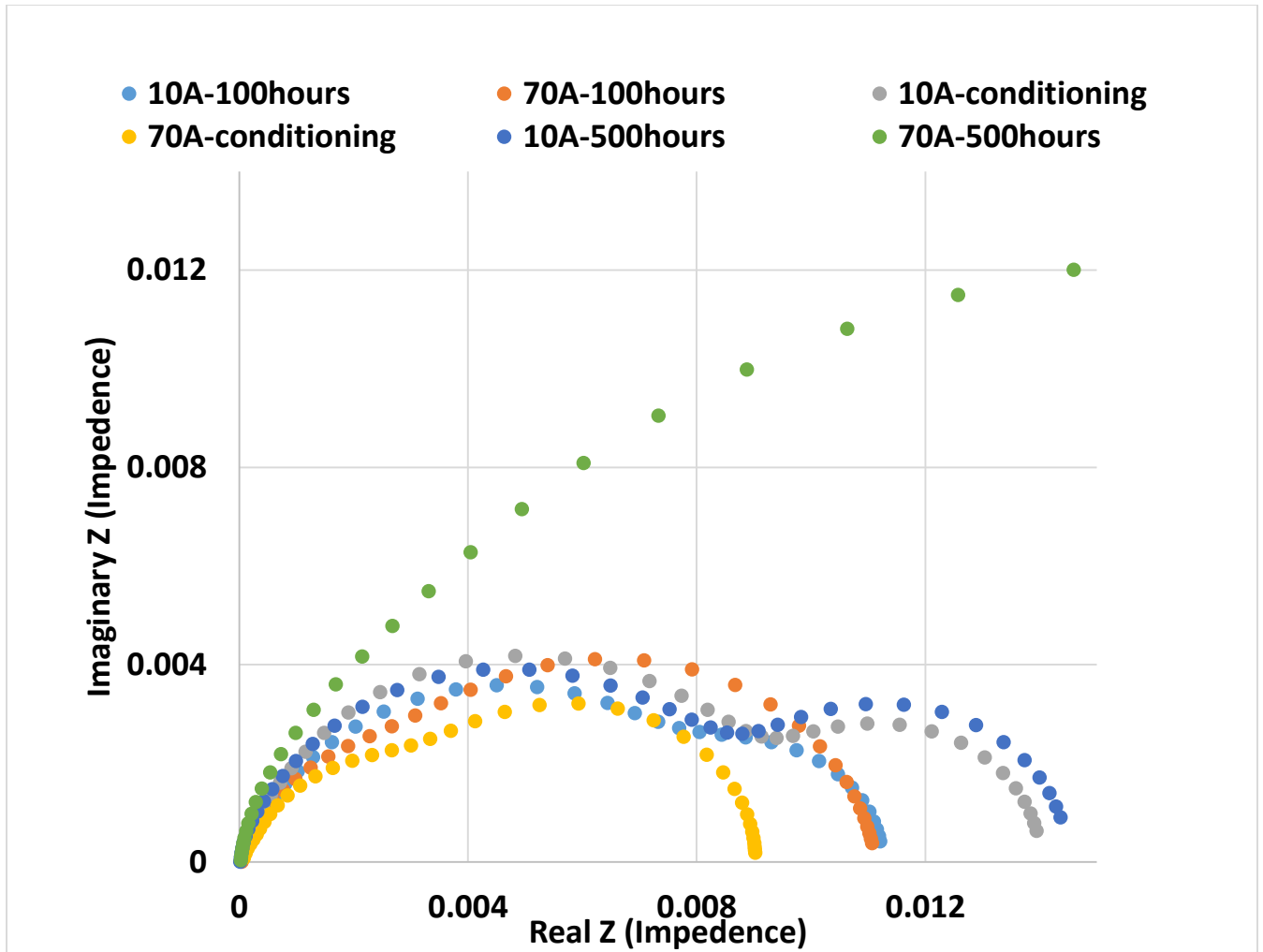
Figure 18: Solvicore EIS Spectra

The spectra clearly shows the degradation occurring with increasing cycling. It also shows that the majority of the degradation occurs in the mass transport losses at high current. The cathode activation losses increase slightly over the stress test but become completely overwhelmed by mass transport losses at 70A after 500 hours of cycling. The spectra for CEA-Grenoble, shown in Figure 19, shows similar degradation but not to the same extent.
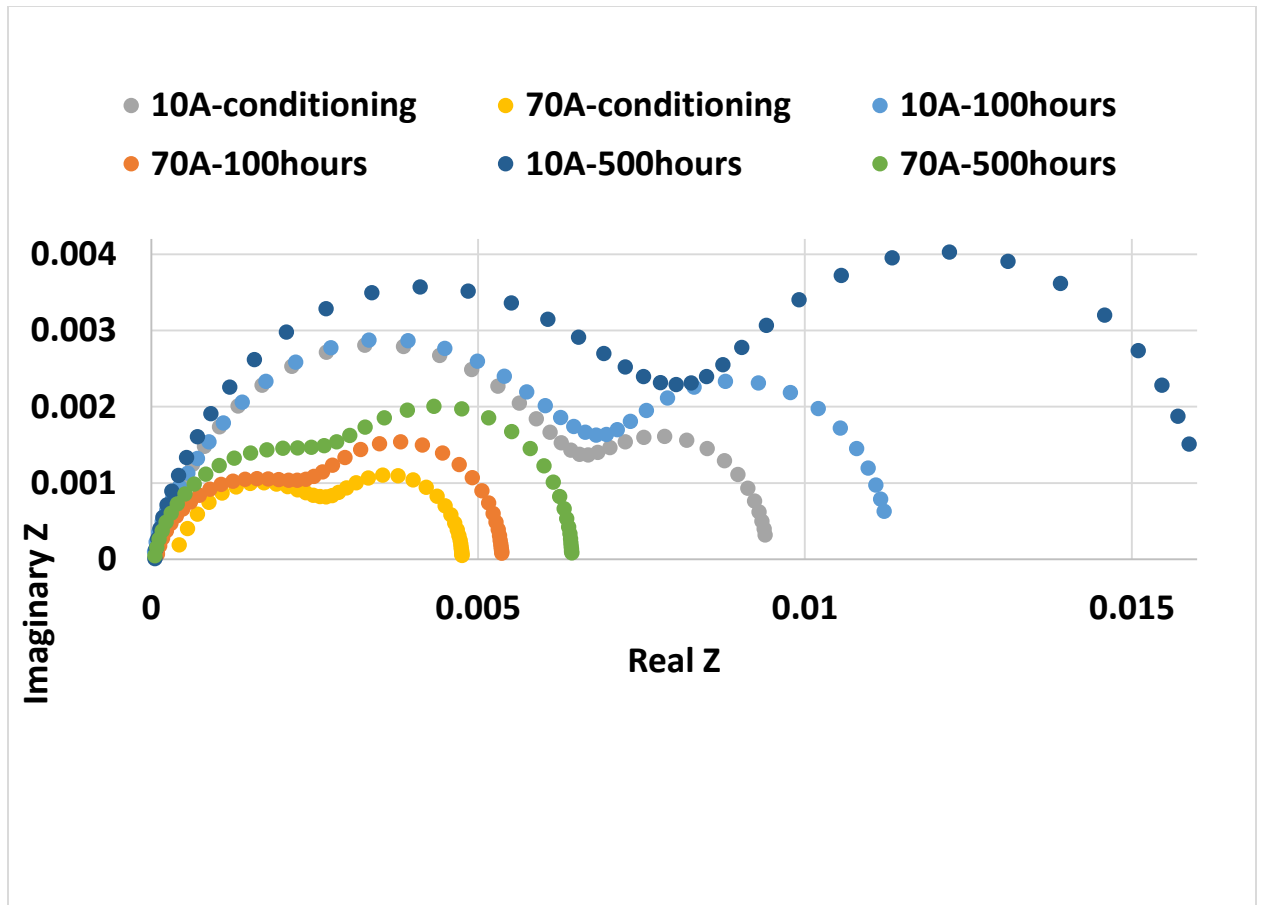
Figure 19: CEA-Grenoble EIS Spectra

For the CEA Grenoble EIS spectra, the regions are very distinct between the cathode activation losses and the mass transport losses. In order to more accurately assess the different parameters, the EIS data is fit through a specialized excel program.

GEIS: Ohmic Resistance
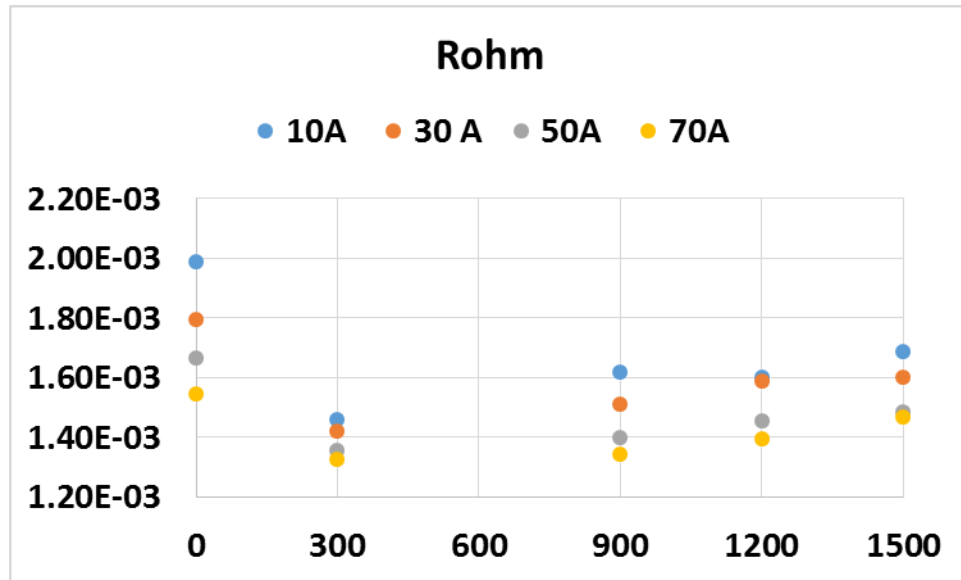
Figure 20: Ohmic Resistance of Solvicore MEA

The MEA shows a continued conditioning process, reducing the ohmic resistance throughout the first 100 hours of cycling. The MEA then continues to become more resistant to charge transfer throughout all layers of the PEM fuel cell. This increasing ohmic resistance is responsible for the increasing slope present in the polarization curves in Figure 13, especially with increasing current. The ohmic resistance of the MEA provided by CEA-Grenoble exhibits a much different trend. In Figure 21, the graph shows that the ohmic resistance increases with cycling tests at 10A, but decreases for 30, 50, and 70 amps.
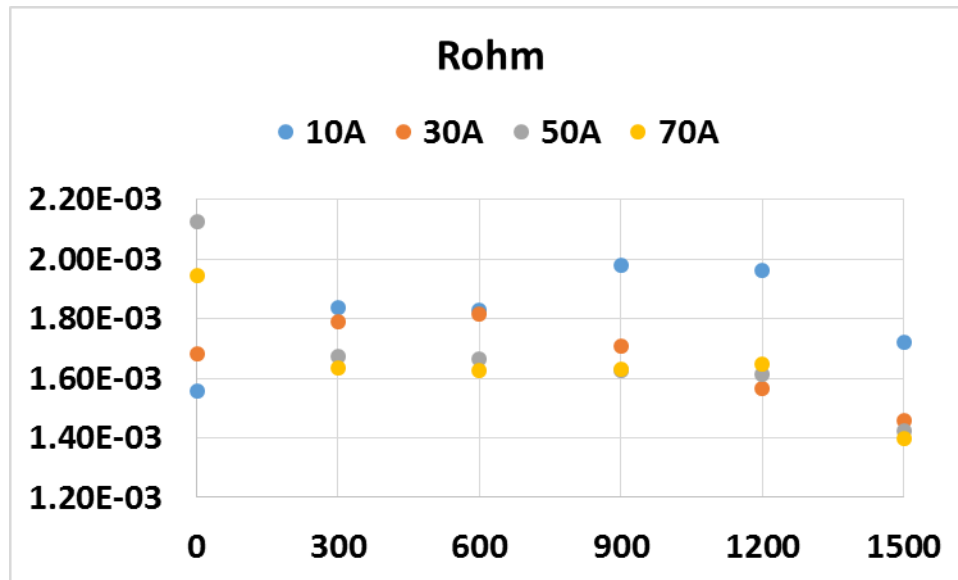
Figure 21: Ohmic Resistance of CEA-Grenoble MEA

This reduction in current shows resilience of the GDL, maintaining enough carbon to sustain electron transport without degradation. The improvement may be related to a the fine balance of water between the membrane and catalyst layer, at higher currents the water produced increases the kinetic reaction rate of hydrogen transport from the membrane to the catalyst sites in the adjoining layer. As the MEA degrades, the water management properties of the GDL deteriorate to a level where water is being moved out to prevent mass transport losses, but due to degradation the GDL leaves water behind, resulting in the reduced ohmic resistance.

GEIS: Cathode Charge Resistance

The cathode charge resistance or activation losses are pretty consistent throughout both membranes. The solvicore EIS data shows a dramatic increase in cathode activation losses, but this is due to the overwhelming influence of mass transport losses and an error of the excel fitting program. The cathode activation losses are not sufficiently degraded over the course of the cycling stress test.
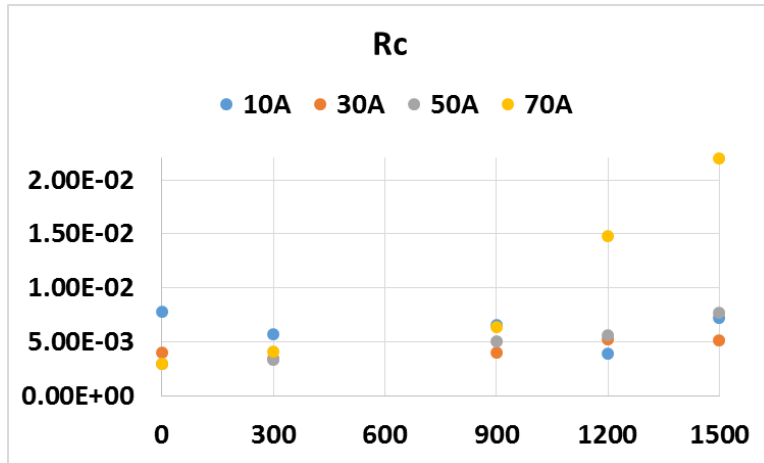
Figure 22: Solvicore Cathode Activation Losses
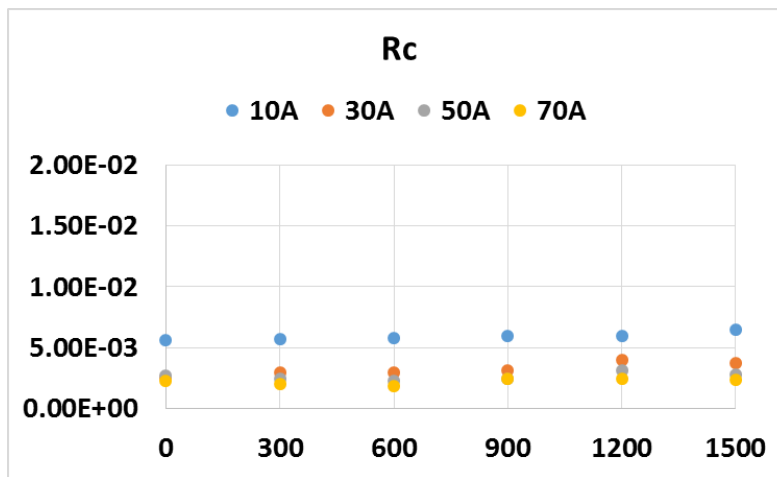
Figure 23: CEA-Grenoble Cathode Activation Losses

GEIS: Mass Transfer Losses

Accumulation of water inhibits the transport of oxygen molecules to the catalyst sites. EIS data shows that the diffusion resistance increases with cycling. The Solvicore MEA exhibited the most mass transfer resistance as shown in Figure 24.
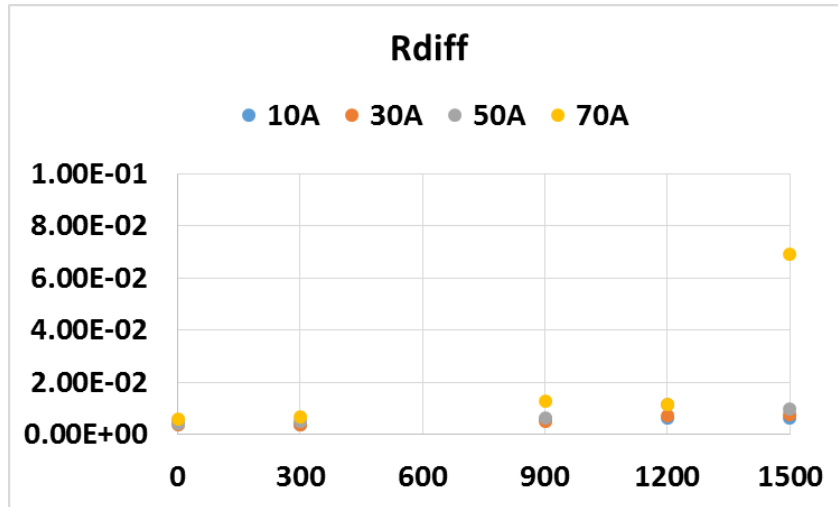
Figure 24: Solvicore Mass Transfer Resistance

The CEA-Grenoble MEA exhibited about 12% of the same mass transfer resistance, as shown in Figure 24. However, when comparing the performance at the same current, the mass transport losses are only 5-6%, this is the most powerful contributor to the performance of the fuel cell at higher current as shown in Figure 14.
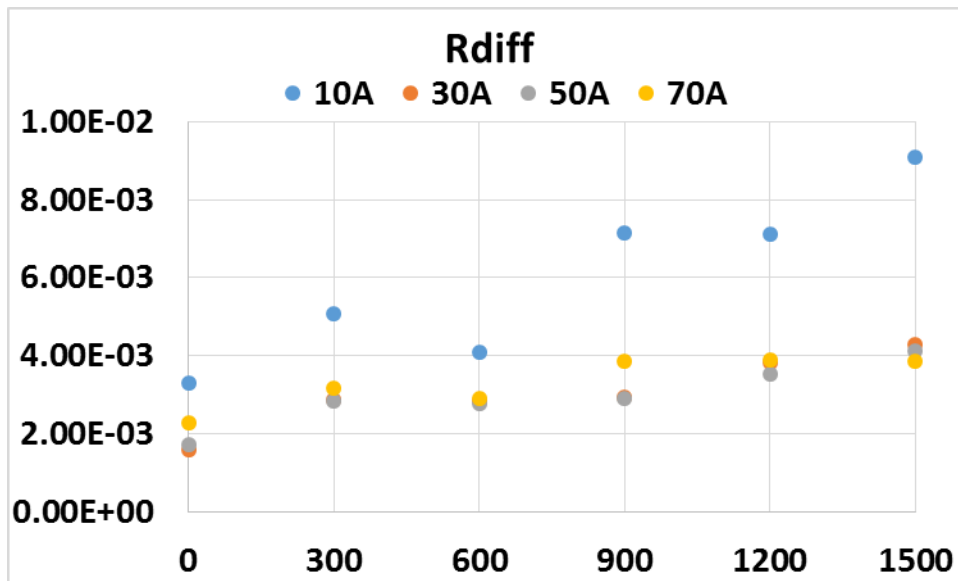
Figure 25: CEA-Grenoble Mass Transport Resistance

Linear Sweep Voltammetry
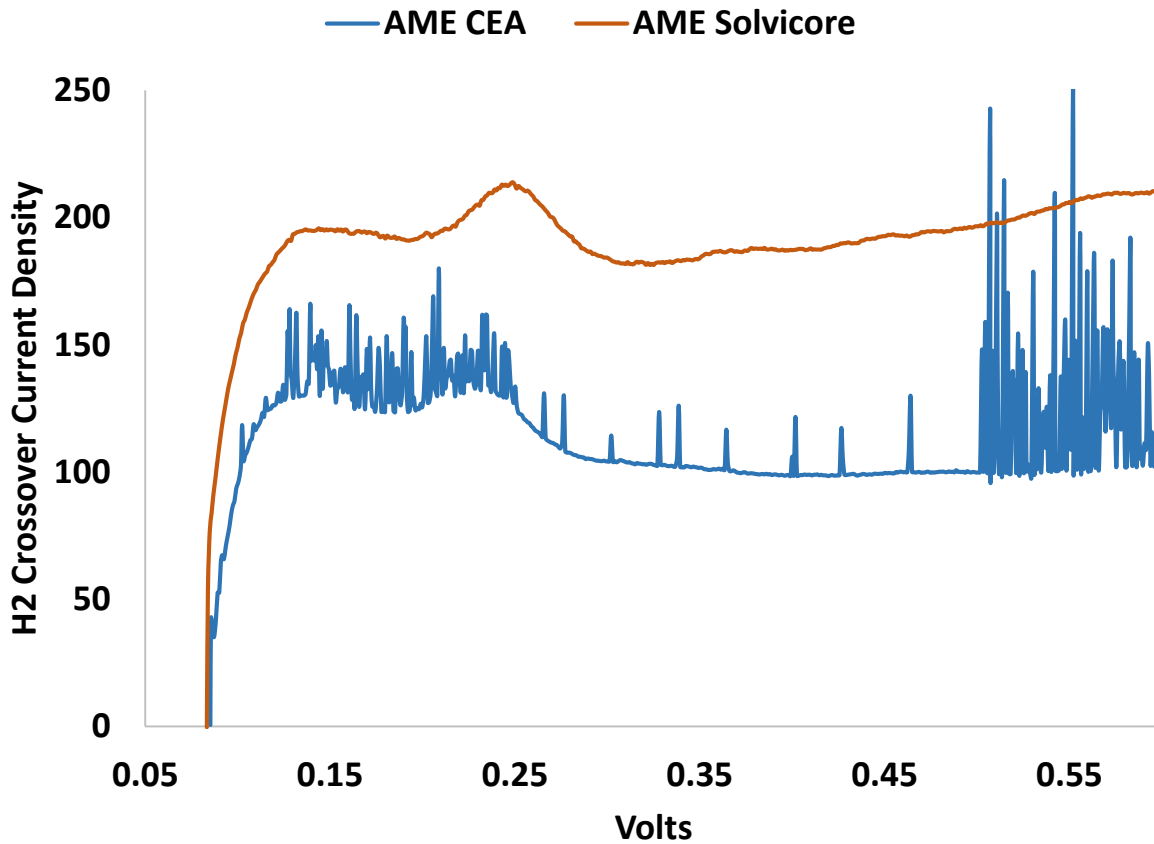
Figure 26: Linear Sweep Voltammetry Comparison; Note: AME = Assemblage membrane-électrode or MEA in French

The Linear Sweep Voltammetry shows that the membrane for the CEA-Grenoble developed

holes in the membrane which permitted excessive hydrogen crossover. The cause of these holes

were undetermined, but the performance of the CEA-Grenoble still allowed for analysis of the

performance of the gas diffusion layer. The impact of the hydrogen crossover is presented in Table

1.

Table 2: Hydrogen Crossover

MEA	Conditioning	500 hours
CEA-Grenoble	~2 mA/cm^2	>100 mA/cm^2
Solvicore	~2 mA/cm^2	<3 mA/cm^2

This increase of hydrogen crossover explains the drop in open circuit voltage shown in the cycling results of CEA-Grenoble in Figure 13.

Cyclic Voltammetry

Cyclic Voltammetry assess the total active surface area of the catalyst inside the fuel cell. Figure 27 plots the CV results of the CEA-Grenoble and Solvicore MEAs.
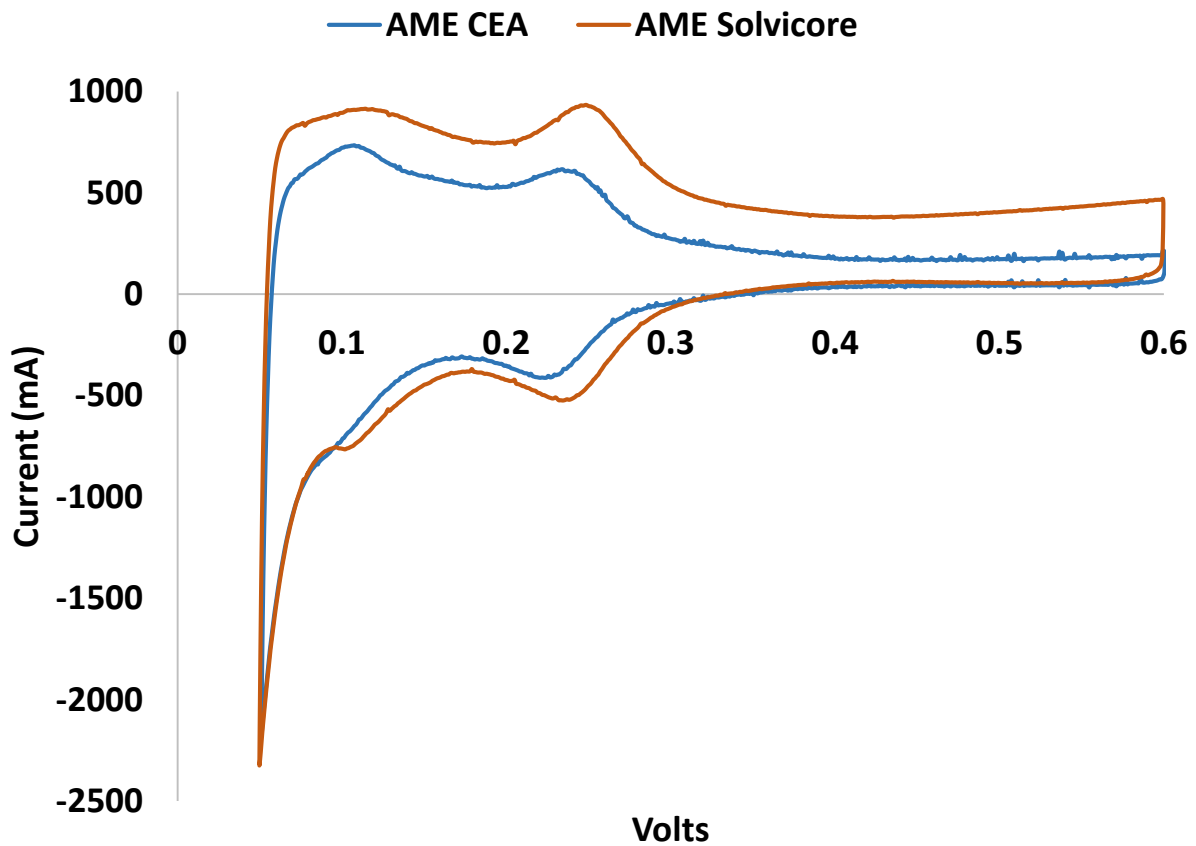
Figure 27: Cyclic Voltammetry Results

After analysis, the total surface area of platinum per surface area (cm^2Pt/cm^2) of the catalyst layer is calculated. These results are compared in Figure 28.
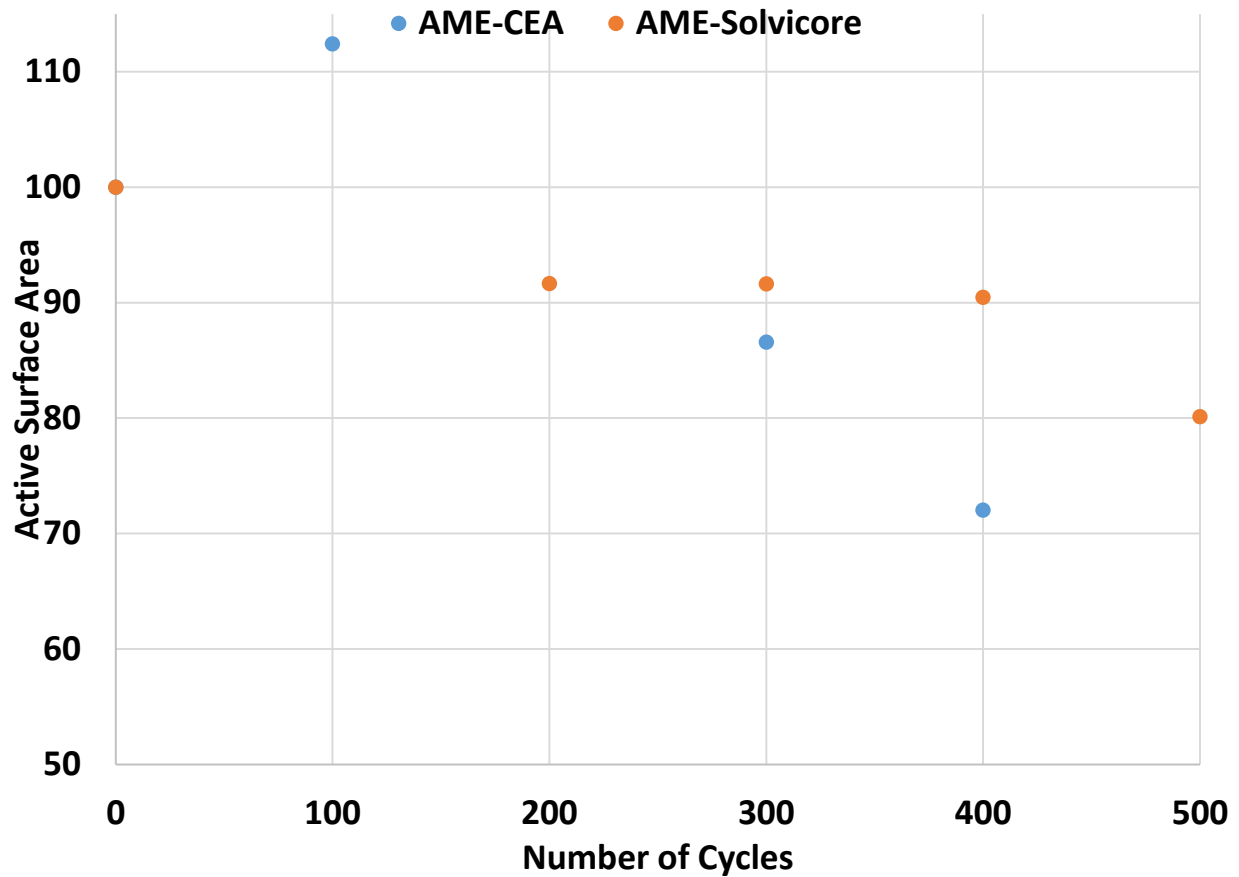
Figure 28: Electrochemical Surface Area

Both samples demonstrated a reduction of active surface area of the platinum catalyst. This occurs through "clumping" of the Pt nanoparticles. While the reduction is present, it is normal for operation of a fuel cell and the contribution to the fuel cell performance after extended use is dwarfed by the influence of the GDL at higher currents.

Carbon Corrosion

A determination of the effect on fuel cell performance by carbon corrosion was attempted through in situ testing of the GDLs in the 7.5 cm^2 fuel cell with a constant voltage of 1.2 volts applied. The CP tests, performed every 24 hours, were used to create polarization curves that

illustrated the overall performance of the cell. An overlay of all of the polarization curves can be found below.
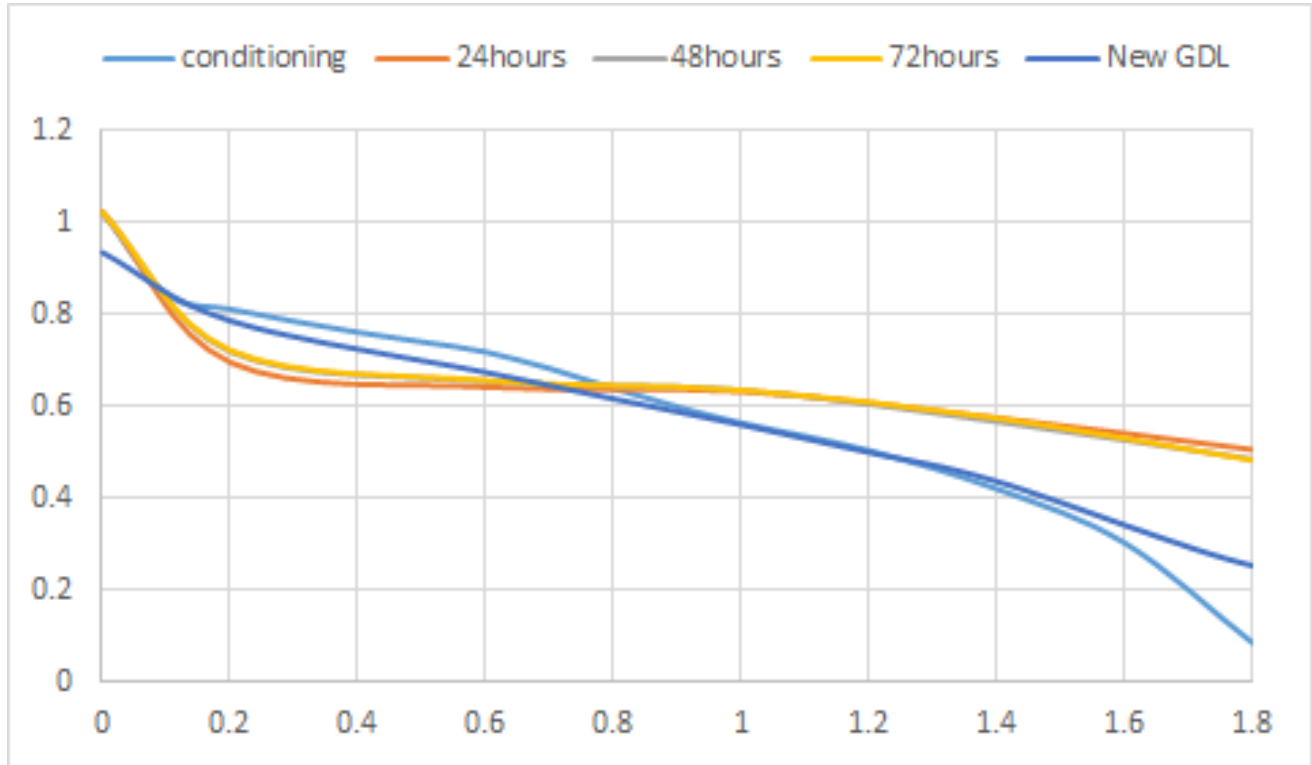
Figure 29: Carbon Corrosion Polarization Curves

By comparing the polarization curves from different 24-hour periods of the carbon corrosion test, it was hoped that some insight could be gleaned into how the presence a high potential across the cell could cause carbon corrosion, thereby reducing the cell's performance. However, the data collected from this experiment did not provide the expected result. The graph above shows an improvement in cell performance at longer time intervals under stress conditions. While activation losses do increase significantly by 24 hours of exposure, the ohmic losses of the cell are simultaneously greatly reduced. This can be seen in the middle section of the graph where the polarization curves from the later times are quite level.

The increase in overall performance of the cell after exposure to high potential can most likely be attributed to the MEA not being fully conditioned before the testing commenced. If this were the case, the initial readings would be of the cell before it had achieved maximum performance. While the testing proceeded, the cell would have continued to mature which would cause its performance to improve. The improvement in performance from MEA maturation has the capacity to overcome the negative effects of carbon corrosion caused by the voltage potential. Therefore, the results from this test were deemed inconclusive. We recommend repeating the test with a focus on ensuring that the MEA is properly conditioned beforehand.

Ex Situ Degradation

The GDLs degraded in ex situ experiments (electrochemical degradation and immersion) were placed on the cathode side of the 7.5 cm^2 fuel cell. Each degraded GDL was tested independently to determine the varying effects of different stress conditions on fuel cell performance. CP was performed and polarization curves were created from the resulting data for each GDL. An overlay of the polarization curves can be found below.
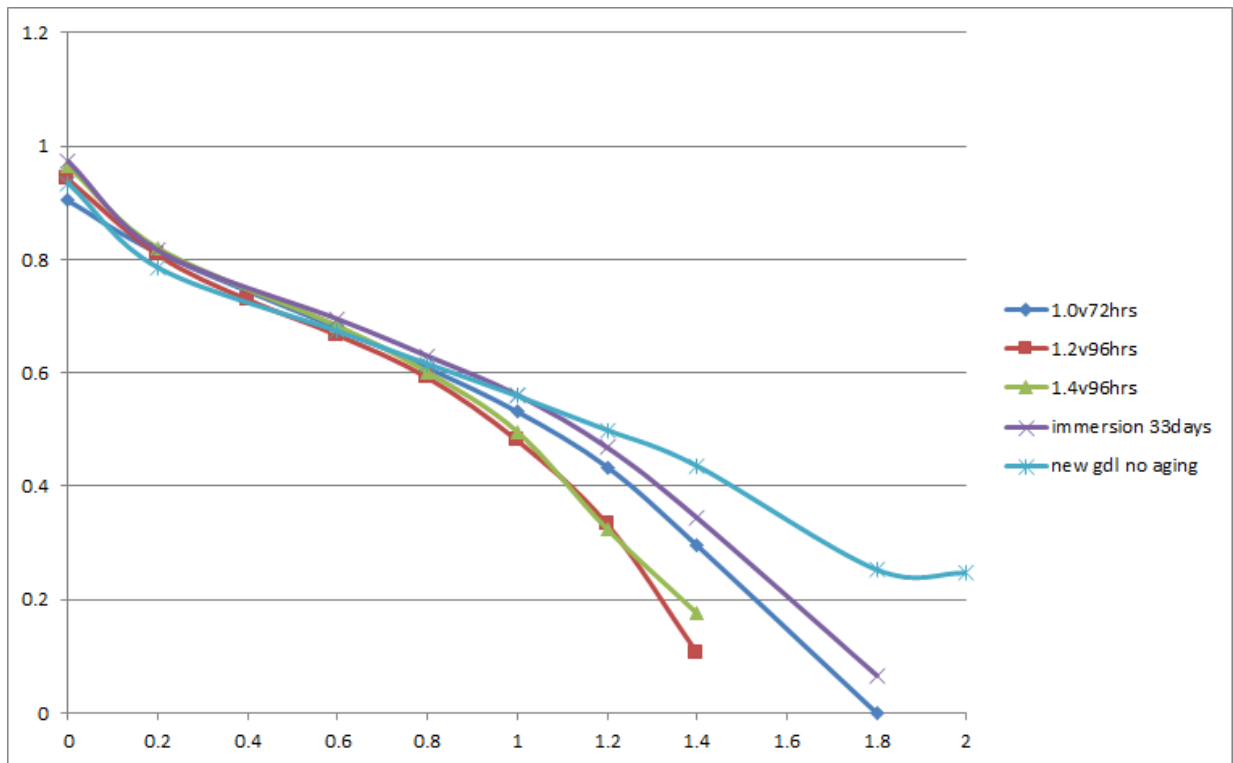
Figure 30: Ex Situ Degradation Polarization Curves

The above graph illustrates the approximate performance of the cells with the different GDLs. With each GDL having been exposed to varying types and levels of stress conditions, the ex situ testing was useful in showing what type of stressors caused the greatest reduction in fuel cell performance. The results of these tests show that, regardless of the kind of exposure to the GDL, activation losses and ohmic losses remain mostly unaffected. This is to be expected because activation losses depend on the condition of the catalyst layer and the number of active sites available for the reactions to take place, while ohmic losses are caused by a resistance to the flow of electrons across the cell. Neither of these should be adversely affected by the targeted degradation of the GDLs undergone in these tests.

The striking difference between the performances of the respective GDLs occurred at the right end of the polarization curves. This section represents the mass transport losses, with a steeper

decline equating to greater mass transport loss. Each cell using a degraded GDL shows a marked increase in mass transport losses compared to the cell using a non-degraded GDL. These findings indicate that degradation of the GDL results in greater mass transport losses in the cell, resulting in decreased performance.

Regarding the differing effects of various stressors on the GDLs, the data make it clear that voltage plays an outsized role in the degradation of GDLs. A GDL immersed in a solution of 1.0 M H_2SO_4 for 33 days performed better than GDLs immersed in a solution of 0.5 M H_2SO_4 and exposed to varying levels of voltage for four days (note in the graph that the GDL exposed to 1.0 volts was degraded for three days, rather than the intended four, due to the final sample being too damaged to properly test). The exposure to acid appears to be a relatively small factor in terms of degradation, with increases in voltage directly correlating to greater levels of GDL degradation and mass transport losses.

The GDLs were tested further using EIS. The results from these tests, shown in Figure 31, support the findings from the polarization curves. The increasing arcs on the right side of the EIS graphs indicate increasing mass transport resistance. The positive correlation between the level of voltage exposed to the GDL and mass transport resistance is supported by the data from both the polarization curves and the EIS data.
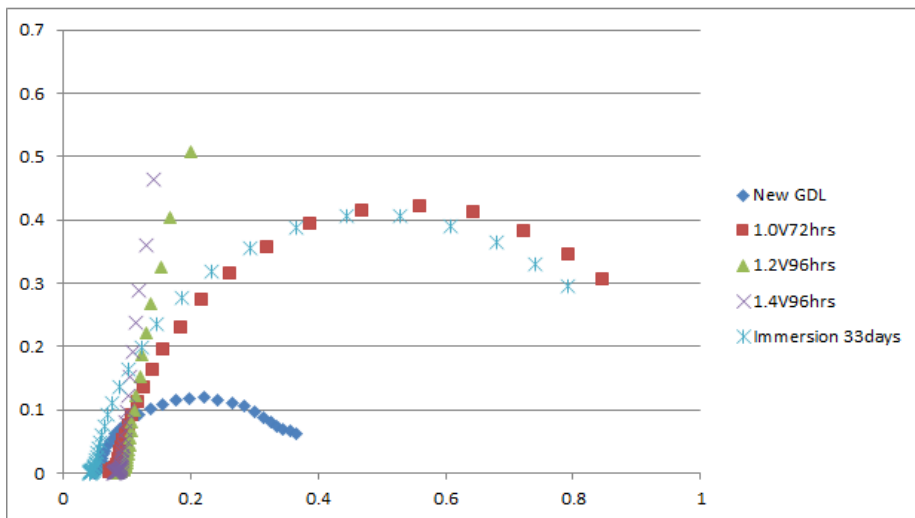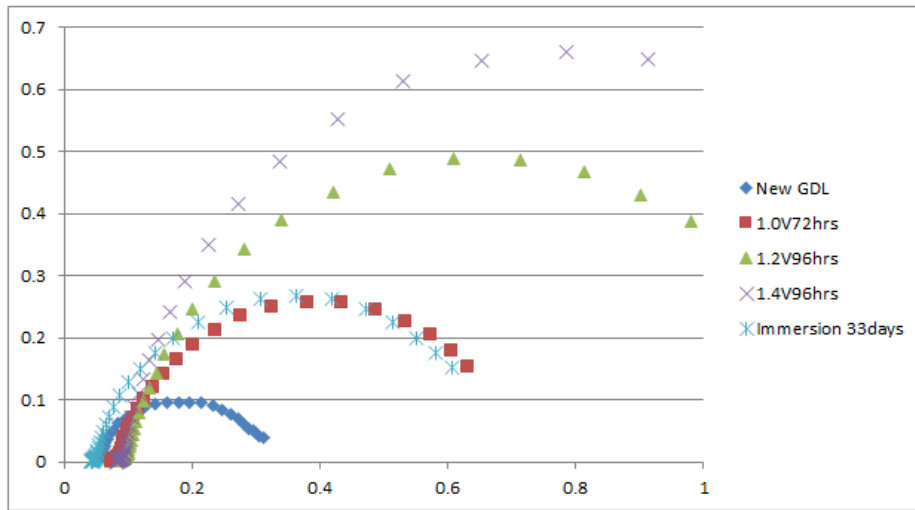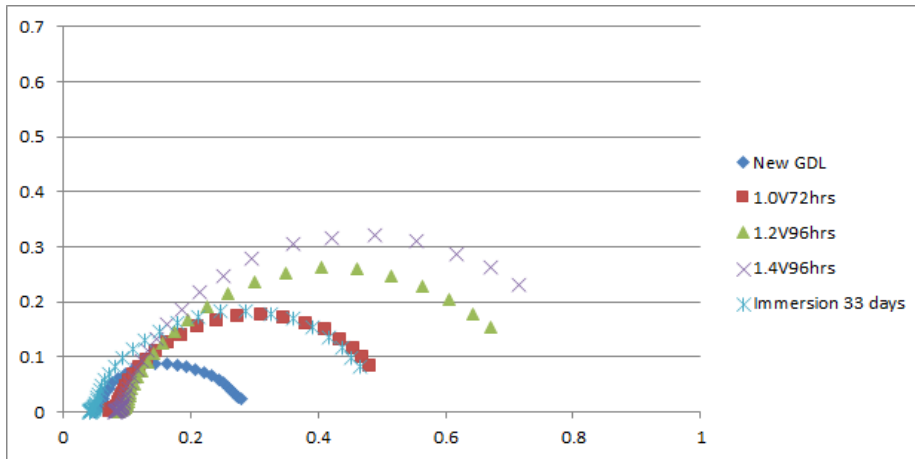
Figure 31: Ex Situ Degradation EIS (1.0 A, 1.2 A, 1.4 A)

Conclusions

From the data presented above, it can be concluded that the main cause of GDL degradation is the presence of high voltage potential across the fuel cell. This appears to have an adverse effect on the integrity of the GDL, causing drastic increases in mass transport losses. When compared to other layers of the MEA, GDL degradation was found to cause the most significant reduction in cell performance. When the GDL, especially the microporous layer, breaks down due to carbon corrosion caused by the high-potential-induced oxidation of carbon, it loses its ability to effectively remove the water being produced at the cathode-side catalyst layer. The microporous layer of the GDL normally induces capillary pressure that pushes the water away from the MEA and out of the cell. When the GDL breaks down, the capillary pressure is lost and water builds up in the MEA. This buildup of water inhibits oxygen molecules from diffusing through the GDL and onto the catalyst layer, effectively drowning the cell. Maintaining the structural integrity of the GDL is imperative for effective water removal at the cathode. Without effective water removal, the rate of the oxidation reaction at the cathode-side catalyst layer is greatly reduced, diminishing the overall performance of the fuel cell.

To combat the issue of GDL degradation caused by high potential, more research must be done to determine how to either minimize a fuel cell's exposure to drastic changes in voltage or develop a GDL structure more resistant to such stress conditions. LRGP is currently researching several avenues to accomplish this objective. This research includes implementing variable levels of PTFE throughout the GDL to make the material properties more resilient. There is also a promising new approach currently being researched at LRGP that would greatly reduce the stress felt by the fuel cell from sudden changes in voltage. Researchers are connecting a capacitor to a fuel cell to act as a buffer to rapid changes in current demands by the system. The presence of a capacitor acts as a

buffer to rapid changes in current demands by the system, allowing the fuel cell to gradually step up or down its output of current, with the capacitor supplying or absorbing the current difference between the supply and demand. It is possible that this new approach will lessen the stress felt by the GDL and minimize the carbon corrosion within the cell.

This research has determined that GDL integrity is vital to the health and performance of a fuel cell and that the main cause of GDL degradation is high cell potential. Further research should be conducted to combat this issue in order to improve the longevity and durability of PEMFC technology, making it an economically viable alternative to combustion engines and battery-powered EVs for automotive applications.

References

Barbir, Frano. 2013. *PEM Fuel Cells - Theory and Practice.* Waltham: Elsevier.

Belhadj, Mariem. 2016. "Personal Correspondance."

Bott, Adrian W. n.d. *Controlled Current Techniques.* Accessed February 19, 2016.
    http://www.currentseparations.com/issues/18-4/pdf/bott.pdf.

Chen, Guobao, Huamin Zhang, Haipeng Ma, and Hexiang Zhong. 2009. "Electrochemical
    Durability of Gas Diffusion Layer Under Simulated Proton Exchange Membrane Fuel Cell
    Conditions." *International Journal of Hydrogen Energy* 8185-8192.

n.d. *Chronopotentiometry.* Accessed February 19, 2016.
    https://www.basinc.com/mans/EC_epsilon/Techniques/CPot/cp.html.

Cultura, A., and Z. Salameh. 2014. "Dynamic Analysis of a Stand Alone Operation of PEM Fuel
    Cell System." *Journal of Power and Energy Engineering* 1-8.

Dale, N. V., M. D. Mann, H. Salehfar, A. M. Dhirde, and T. Han. 2010. "Impedance Study of a
    Proton Exchange Membrane Fuel Cell Stack Under Various Loading Conditions." *Journal of
    Fuel Cell Science and Technology.*

Lapicque, Francois. 2016. "Personal Correspondance."

Larminie, James, and Andrew Dicks. 2003. *Fuel Cell Systems Explained.* West Sussex: John Wiley &
    Sons Ltd.

n.d. *Nafion Store.* Accessed February 24, 2016. http://www.nafionstore.com.

Rao, R. M., and R. Rengaswamy. 2006. "A Distributed Dynamic Model for Chronoamperometry,
    Chronopotentiometry, and Gas Starvation Studies in PEM Fuel Cell Cathode." *Chemical
    Engineering Science* 7393-7409.

Smithsonian Institution. n.d. "Fuel Cell Origins." *Smithsonian Institution.* Accessed February 17, 2016.
    http://americanhistory.si.edu/fuelcells/origins/origins.htm.

—. n.d. "PEM Fuel Cells." *Smithsonian Institution.* Accessed February 17, 2016.
    http://americanhistory.si.edu/fuelcells/pem/pemmain.htm.

Song, Chaojie, Chris Jensen Chua, Yanghua Tang, JianLu Zhang, Jiujun Zhang, Jing Li, Keping
    Wang, Scott McDermid, and Paul Kozak. 2008. "Voltage Jump During Polarization of a
    PEM Fuel Cell Operated at Low Relative Humidities." *International Journal of Hydrogen Energy*
    2802-2807.

Wu, Jinfeng, Xiao Zi Yuan, Haijiang Wang, Mauricio Blanco, Jonathan J. Martin, and Jiujun Zhang.
    2008. "Diagnostic Tools in PEM Fuel Cell Research: Part I Electrochemical Techniques."
    International Journal of Hydrogen Energy 1735-1746.

Appendix

Note: To view all data used in the completion of this paper, please refer to the LRGP lab at ENSIC/University of Lorraine in Nancy, France. Data collection was under the advisement of François Lapicque and Mariem Belhadj.

Large cell CV
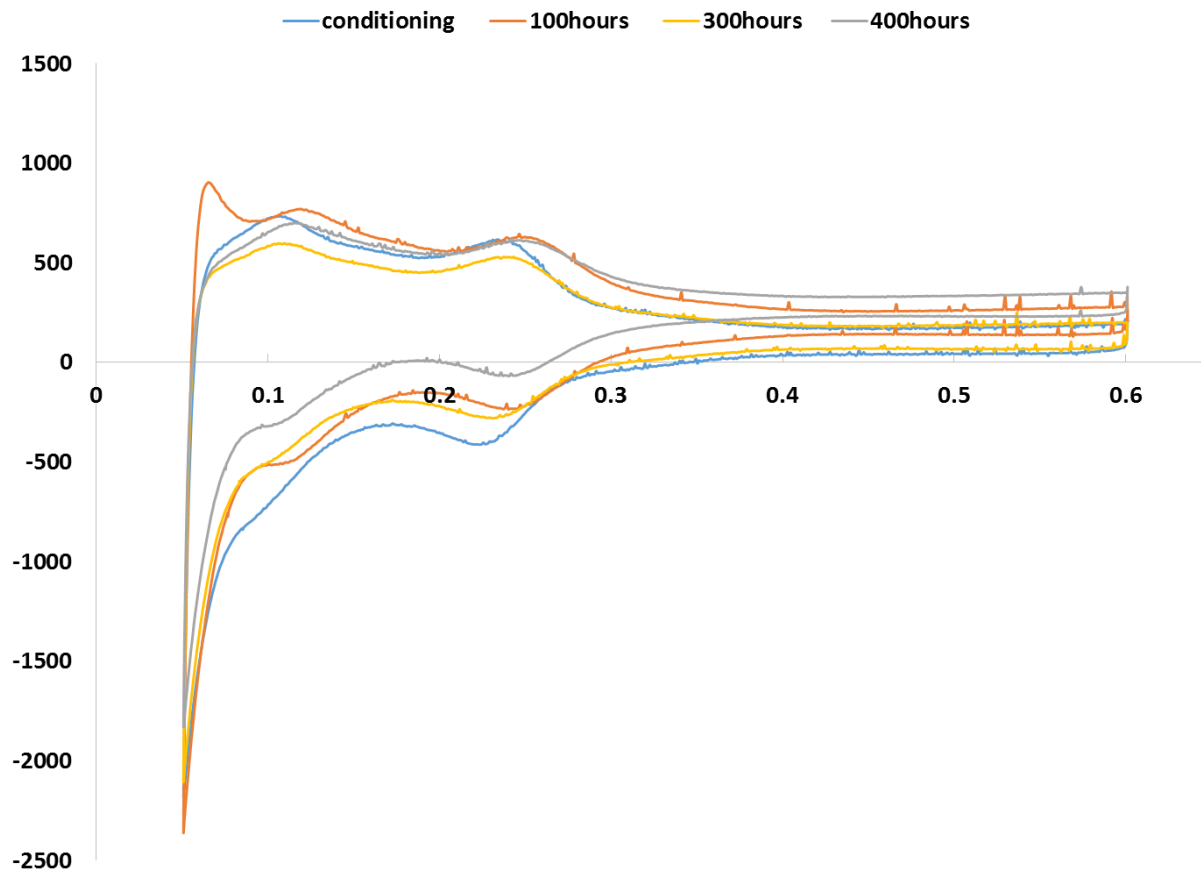
Large cell LSV
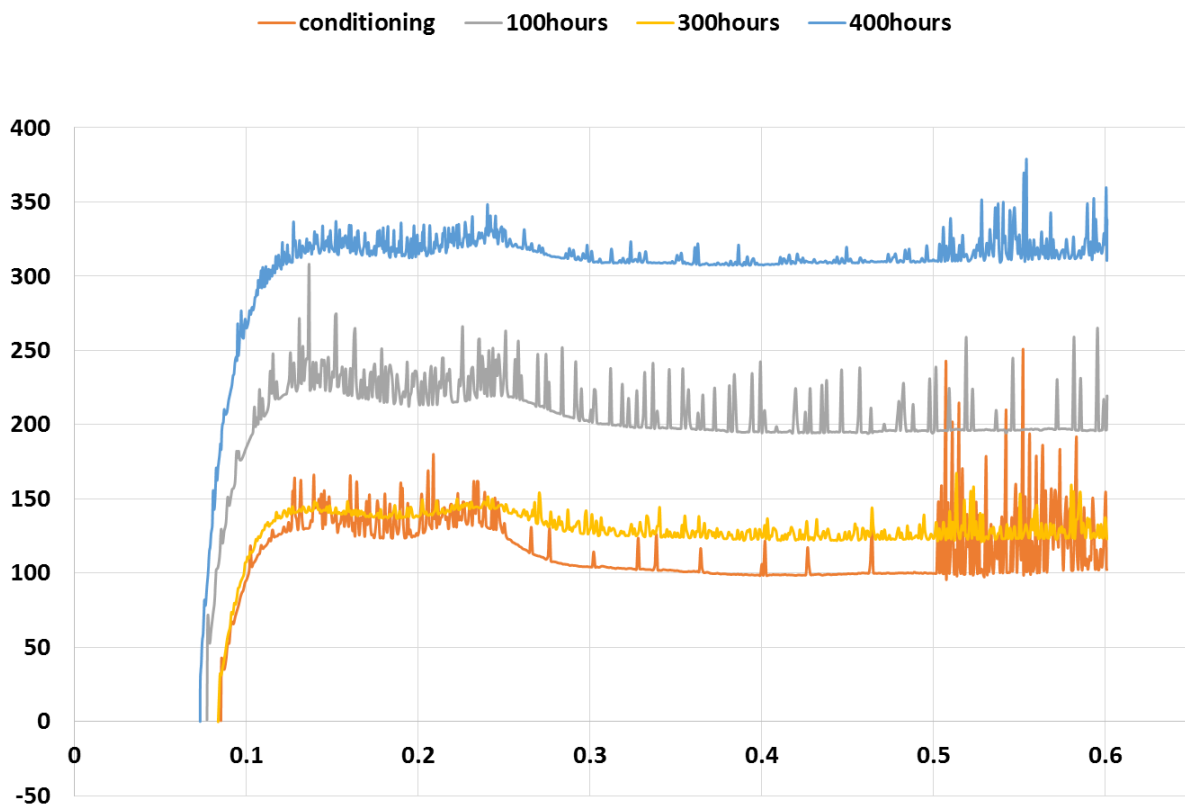
Large cell – EIS model – 100 hours
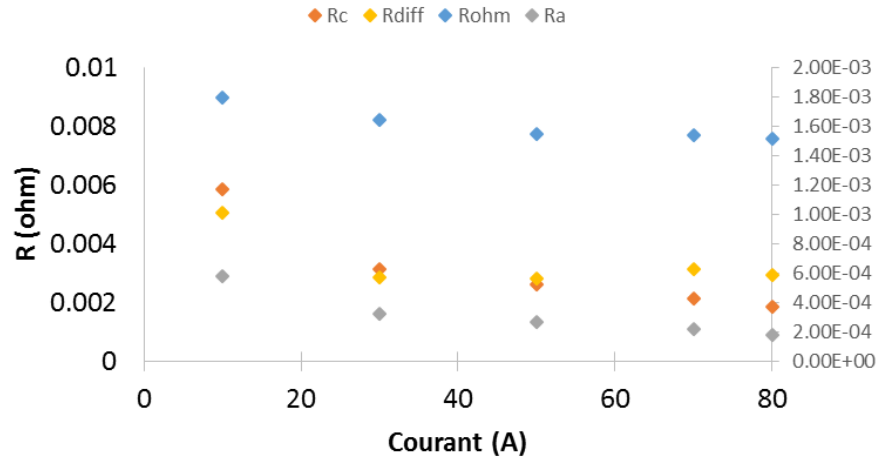
Large cell – EIS model – 400 hours